Original Article

MOLECULAR METABOLISM

LANCL1 binds abscisic acid and stimulates glucose transport and mitochondrial respiration in muscle cells *via* the AMPK/PGC-1α/Sirt1 pathway

Sonia Spinelli [1,5], Giulia Begani [1,5], Lucrezia Guida [1], Mirko Magnone [1], Denise Galante [2], Cristina D'Arrigo [2], Claudia Scotti [3,4], Luisa Iamele [3,4], Hugo De Jonge [3,4], Elena Zocchi [1,*], Laura Sturla [1]

ABSTRACT

Objective: Abscisic acid (ABA) is a plant hormone also present and active in animals. In mammals, ABA regulates blood glucose levels by stimulating insulin-independent glucose uptake and metabolism in adipocytes and myocytes through its receptor LANCL2. The objective of this study was to investigate whether another member of the LANCL protein family, LANCL1, also behaves as an ABA receptor and, if so, which functional effects are mediated by LANCL1.

Methods: ABA binding to human recombinant LANCL1 was explored by equilibrium-binding experiments with [^{3}H]ABA, circular dichroism, and surface plasmon resonance. Rat L6 myoblasts overexpressing either LANCL1 or LANCL2, or silenced for the expression of both proteins, were used to investigate the basal and ABA-stimulated transport of a fluorescent glucose analog (NBDG) and the signaling pathway downstream of the LANCL proteins using Western blot and qPCR analysis. Finally, glucose tolerance and sensitivity to ABA were compared in LANCL2$^{-/-}$ and wild-type (WT) siblings.

Results: Human recombinant LANCL1 binds ABA with a K_d between 1 and 10 μM, depending on the assay (i.e., in a concentration range that lies between the low and high-affinity ABA binding sites of LANCL2). In L6 myoblasts, LANCL1 and LANCL2 similarly, i) stimulate both basal and ABA-triggered NBDG uptake (4-fold), ii) activate the transcription and protein expression of the glucose transporters GLUT4 and GLUT1 (4-6-fold) and the signaling proteins AMPK/PGC-1α/Sirt1 (2-fold), iii) stimulate mitochondrial respiration (5-fold) and the expression of the skeletal muscle (SM) uncoupling proteins sarcolipin (3-fold) and UCP3 (12-fold). LANCL2$^{-/-}$ mice have a reduced glucose tolerance compared to WT. They spontaneously overexpress LANCL1 in the SM and respond to chronic ABA treatment (1 μg/kg body weight/day) with an improved glycemia response to glucose load and an increased SM transcription of GLUT4 and GLUT1 (20-fold) of the AMPK/PGC-1α/Sirt1 pathway and sarcolipin, UCP3, and NAMPT (4- to 6-fold).

Conclusions: LANCL1 behaves as an ABA receptor with a somewhat lower affinity for ABA than LANCL2 but with overlapping effector functions: stimulating glucose uptake and the expression of muscle glucose transporters and mitochondrial uncoupling and respiration *via* the AMPK/PGC-1α/Sirt1 pathway. Receptor redundancy may have been advantageous in animal evolution, given the role of the ABA/LANCL system in the insulin-independent stimulation of cell glucose uptake and energy metabolism.

Keywords LANCL1; Abscisic acid; Glucose transporters; UCP3; Sarcolipin; Cell respiration

1. INTRODUCTION

The lanthionine synthase C-like proteins (LANCL proteins) are the mammalian homologs of bacterial LanC enzymes, which catalyze the addition of the thiol of Cys to dehydrated Ser in the biosynthesis of lanthionine-containing peptides (lanthipeptides), with antibiotic properties. The mammalian LANCL protein family contains three members, LANCL1, LANCL2, and LANCL3, encoded on chromosomes 2, 7, and X, respectively [1,2]. As the triple knockdown of these proteins does not reduce the brain content of a downstream metabolite of lanthionine, lanthionine ketimine, it has been concluded that mammalian LANCL proteins are not involved in lanthionine synthesis [3], leaving their role in mammalian physiology open to investigation.

[1]Department of Experimental Medicine, Section of Biochemistry, School of Medical and Pharmaceutical Sciences, University of Genova, Viale Benedetto XV 1, 16132, Genova, Italy [2]Institute for Macromolecular Studies, National Research Council, Via De Marini 6, 16149, Genova, Italy [3]Department of Molecular Medicine, Immunology and General Pathology Unit, University of Pavia, Via Ferrata 9, 27100, Pavia, Italy [4]Ardis Srl, Via Taramelli 24, 27100, Pavia, Italy

[5] These authors contributed equally to this work.

*Corresponding author. E-mail: ezocchi@unige.it (E. Zocchi).

Received April 10, 2021 • Revision received May 28, 2021 • Accepted May 28, 2021 • Available online 5 June 2021

https://doi.org/10.1016/j.molmet.2021.101263

LANCL2 has been shown to bind abscisic acid (ABA), a plant hormone and mammalian regulator of cell glucose uptake and metabolism [4,5]. LANCL2 shares properties typical of a peptide and steroid hormone receptor; though not a transmembrane protein, as it is bound to the intracellular side of the plasmamembrane through a myristoyl anchor [6], it activates a G protein upon ABA binding and is capable of nuclear translocation [7], a typical feature of steroid hormone receptors. Downstream of LANCL2, ABA stimulates muscle glucose transports in an insulin-independent manner *via* activation of the AMPK/PGC-1α axis [8]. LANCL2 is also an activator of mTORC2 [9] and interacts with PPAR-γ, allowing PPAR-γ-mediated activation of adipogenic genes during insulin-stimulated triglyceride accumulation in white adipocytes [10]. Interestingly, LANCL2 is also involved in the activation of transcription of several browning genes in brown adipocytes *in vitro* and *in vivo* [11]. LANCL2 is ubiquitously expressed, although the highest levels of expression are observed in the brain. As expected from the role of LANCL2 in stimulating muscle and adipocyte glucose transport and metabolism, LANCL2$^{-/-}$ mice show a reduced glucose tolerance [5]. However, unexpectedly, preliminary results showed that LANCL2$^{-/-}$ mice respond to ABA with a significant reduction of the glycemia profile after an oral glucose load [5]. This observation indicates the presence of (an)other ABA receptor(s), in addition to LANCL2, capable of mediating the glycemia-lowering effect of ABA *in vivo*.

An obvious candidate for this role is LANCL1, as it shares a significant sequence identity (54.2%), similar intracellular localization (it is a peripheral membrane protein), and tissue expression pattern with LANCL2. This study aimed at investigating whether LANCL1 could behave as an ABA receptor similarly to LANCL2.

To test this hypothesis, we performed *in vitro* experiments with human recombinant LANCL1 to verify its ABA-binding capacity with several techniques, including equilibrium binding, surface plasmon resonance, and circular dichroism. Next, we tested the effect on the glucose transport of the overexpression of LANCL1, LANCL2, or of the silencing of both proteins in a rat myoblast cell line. Finally, we compared the response to the exogenous ABA of wild-type and LANCL2$^{-/-}$ mice regarding glucose tolerance and muscle expression of LANCL1/2 target genes. Results suggest that LANCL1 shares the ability to bind ABA and to stimulate glucose transport and mitochondrial function with LANCL2 *in vitro* in rat myoblasts and *in vivo* in the skeletal muscle of LANCL2$^{-/-}$ mice by targeting the AMPK/PGC-1α/Sirt1 pathway, leading to the overexpression of the glucose transporters GLUT4 and GLUT1, the skeletal muscle uncoupling proteins UCP3 and sarcolipin, and the NAD^+ synthesizing enzyme NAMPT.

2. MATERIALS AND METHODS

2.1. Vector construction

2.1.1. Cloning of LANCL1 in PGEX-6-P1 vector

Total RNA was extracted from HeLa cells using the RNeasy Micro Kit (Qiagen, Milan, Italy) according to the manufacturer's instructions and reverse transcribed into cDNA using the iScriptTM cDNA Synthesis Kit (Bio-Rad, Milan, Italy). The full-length hLANCL1 cDNA was amplified by PCR using the following primers: 5′-ATTGAATTCATGGCTCAAAGGGCCTTC-3′ (forward-EcoRI restriction site underlined) and 5′-AATCTCGAGTCAGAGTTCAAATGCAGGGAA-3′ (reverse-XhoI restriction site underlined) for the cloning in pGEX-6-P1 vector (GE Healthcare, Milan, Italy). The PCR was performed in 25 µl containing 1 × reaction buffer, 300 µM dNTP, 7.5 pmol of primers, and using 2.5 units of Pfx50™ DNA Polymerase (Thermo Fisher Scientific, Milan, Italy). The PCR reaction profile was 1 cycle at 94 °C for 2 min, 35 cycles at 94 °C for 15 s, 60 °C for 30s, and 68 °C for 1 min with a final extension for 5 min at 68 °C. The PCR products were purified from agarose gel with a QIAEX II Gel Extraction Kit (Qiagen), digested with *Eco*RI and *Xho*I and with *Eco*RI and *Hin*dIII, and cloned into pGEX-6-P1 using a Rapid Ligation Kit (Roche, Milan, Italy). The LANCL1-pGEX-6-P1 vector was purified using Plasmid Mini Kit (Qiagen), sequenced by TibMolbiol (Genova, Italy), and used to transform *E. coli* BL21 and BL21(DE) (Agilent Technologies, Milan, Italy). The recombinant protein produced by bacteria is LANCL1 fused with glutathione S-transferase (GST); after purification, the GST part of the fusion protein is cleaved to yield the final purified LANCL1 protein.

2.1.2. Cloning of LANCL1 and LANCL2 in pBABE vector

The full-length of LANCL1 was amplified from 1 ng of the LANCL1-pGEX-6-P1 vector by PCR using the following primers: 5′-ATTGGATCCATGGCTCAA AGGGCCTTCCCG-3′ (forward-*Bam*HI restriction site underlined) and 5′-AATGAATTCTCAGAGTTCAAATGCAGGGAACC-3′ (reverse-*Eco*RI restriction site underlined) for the cloning in the pBABE vector (Addgene, MA, USA). The full-length of hLANCL2 was amplified from 1 ng of the LANCL2-pGEX-6-P1 vector [4] by PCR using the following primers: 5′-ATTGAATTC ATGGGCGAGACCATGTCAAAGAG-3′ (forward-*Eco*RI restriction site underlined) and 5′-AATGTCGACTTAATCCCTCTTCGAAGAGTCAAG-3′ (reverse-*Xho*I restriction site underlined) for the cloning in the pBABE vector (Addgene). The PCR amplification, digestion with restriction enzymes, purification of PCR products, and cloning in the pBABE vector were performed as described for the LANCL1-pGEX-6-P1 vector in paragraph 2.1.1.

2.2. Expression and purification of human recombinant LANCL1

BL21 *E. coli* cells containing vectors with the correct inserts were initially cultured in a Luria—Bertani medium (Difco, BD Italia, Roma, Italy) with 200 g/ml ampicillin until the culture reached an A600 of 0.3. LANCL1-GST was expressed by adding isopropyl-b-D-thiogalactopyranoside (final concentration 0.1 mM) and incubating bacteria for 16 h at 20 °C. Cells were harvested by centrifugation and lysed by sonication in 125 mM Tris—HCl, pH 8.0, 150 mM NaCl. After addition of Triton X-100 to a final concentration of 1% and incubation for 30 min at 4 °C, lysates were centrifuged at 10,000 × *g* for 15 min. The LANCL1-GST fusion protein was purified by affinity chromatography using Glutathione (GSH)-Sepharose-4B (GE Healthcare, Milan, Italy) and following the manufacturer's instructions. The release of native LANCL1 was achieved with the PreScission Protease (GE Healthcare) by incubating the GSH-Sepharose-bound fusion protein for 16 h at 4 °C in Tris—HCl pH 7.5, 150 mM NaCl. The PreScission Protease was preemptively activated in the presence of 1 mM DTT (dithiothreitol) for 30 min at 4 °C; the final concentration of DTT in the cleaving incubation was $<$0.5 µM. The protein was concentrated through an Amicon Ultra 30 kDa (Millipore, Milan, Italy). Protein concentrations were determined by the Bradford assay (Bio-Rad), and protein purity was monitored by SDS— PAGE and by gel filtration; gels were stained with ProSieve Blue Protein Staining solution (Lonza, Milan, Italy). Size exclusion chromatography was performed using an HPLC system equipped with a TSKgel G3000SWXL column (Merck, Milan, Italy), with a mobile phase consisting of 50 mM Tris—HCl, pH 7.5 containing 300 mM NaCl, and at a flow rate of 0.7 ml/min. Unrelated negative control-GST fusion recombinant proteins were purified as described above for native LANCL1.

2.3. [^{3}H]ABA binding

The (±)-[^{3}H]-2-cis, 4-trans abscisic acid ([^{3}H]ABA) saturation binding experiments were performed with hLANCL1. Incubations were

performed with 10 μg protein in 150 mM NaCl, 20 mM phosphate buffer pH 7.5, 1 mM EDTA (binding buffer), in a final volume of 100 μL in triplicate for 60 min at 25 °C with 0.05 μM (±)-[^{3}H]ABA (20 Ci/mmol, Biotrend Radiochemicals, Köln, Germany), and in the presence of increasing concentrations of unlabeled (±)-ABA (50 nM–5 mM) (Merck). At the end of incubation, samples were filtered on 0.2 μm-nitrocellulose membranes (Bio-Rad, Milan, Italy); the filters were washed with 3.5 ml of an ice-cold binding buffer and then dried, and the radioactivity was measured in 4.0 ml Ultima-Gold (Perkin Elmer, Italy) with a Packard β-counter. The specific (±)-[^{3}H]ABA binding was calculated as the difference between the total binding and nonspecific binding, obtained with excess unlabeled (±)-ABA (5.0 mM). The maximal binding capacity (B_{max}) and the dissociation constant (K_d) were calculated using the program Saturation Binding, specific binding only, in the GraphPad Prism 5.0 Software (San Diego, CA, USA). In this program, the data are analyzed by nonlinear regression fit.

2.4. Surface plasmon resonance

The direct binding of unlabeled ABA to recombinant hLANCL1 was measured by surface plasmon resonance (SPR) on a Biacore T200 instrument (GE Healthcare) at 25 °C using a CM7 sensor chip (GE Healthcare). First, we evaluated the pre-concentration ability of the chip in a range of pH values compatible with protein stability (10 mM Na acetate, pH 5.5, 5.8, 6.0, 6.5) at a standard concentration (30 μg/ml). The covalent coupling of hLANCL1 was then performed using 10 mM Na acetate pH 5.8 through standard amine coupling. A surface without the immobilized protein was used as a reference channel. All experiments were performed with a running buffer consisting of PBS with the addition of 0.05% Tween 20 (PBS–P) using a flow rate of 30 μl/min. Evaluation of (±)ABA binding to hLANCL1 was performed by injecting ABA dissolved in PBS-P at 1, 2.5, 5, 10, and 20 μM, at a flow rate of 30 μl/min, with a contact time of 30 s, and a dissociation time of 120 s. Bound ABA was removed by a subsequent regeneration step through the injection of 1 M NaCl for 30 s at 30 μl/min. The obtained sensorgrams were used for equilibrium state affinity analysis using the Biacore Evaluation software version 3.1 (GE Healthcare).

2.5. Fluorescence quenching study on the interaction of recombinant LANCL1 with ABA

For quenching titrations, small aliquots of ABA were added to hLANCL1 (8.65 μM) from a stock solution (100 μM) to obtain a molar ratio ranging from 1:2 to 1:450; the fluorescence spectra were recorded after each addition. Fluorescence intensities were corrected for volume changes before further analysis of the quenching data. All emission spectra were recorded on a luminescence spectrometer (PerkinElmer LS50B) at $\lambda_{ex} = 280$ nm (slit width = 5 nm). Absorption measurements were made using a Shimadzu UV-2700 spectrophotometer. To eliminate the inner-filter effects, the fluorescence intensities were corrected by the equation described in [12]. The dynamic quenching constants were determined using the Stern–Volmer equation: $F_0/F = 1+K_{SV}[Q]$, where F_0 and F correspond to the fluorescence intensities of LANCL1 without ABA and with ABA, respectively; [Q] is the concentration of ABA and KSV is the Stern–Volmer quenching constant [13]. The static quenching constant, K_a, and the number of binding sites (n) between LANCL1 and ABA were calculated using the following equation: $\log[(F_0-F)/F] = \log K_a + n \log[Q]$.

2.6. Lentiviral cell transduction

The lentiviral plasmids pLV[shRNA]-Puro-U6 encoding for a control scramble shRNA (shRNA-SCR), for the shRNA targeting rat LANCL1 (shRNA-L1) and the shRNA targeting LANCL2 (shRNA-L2) (plasmid ID: VB010000-0005mme, VB181016-1107sen, VB181016-1124zjp), were purchased from Vector Builder (Chicago, IL, USA). Overexpression of hLANCL1 (ovLANCL1) and hLANCL2 (ovLANCL2) was obtained in rat L6 myoblasts using pBABE vectors constructed as described in 2.1.1, with the empty vector pBABE (Addgene) as negative control (PLV). Lentiviral transductions were performed as described before [14].

2.7. qPCR analysis

Freshly isolated mice quadriceps samples (approx. 30 mg) or L6 cells were incubated with or without 100 nM ABA for the times indicated in the legends. Total RNA was extracted from the muscle using QIAzol Lysis Reagent and Tissue Lyser instrument (Qiagen) and from L6 cells using RNeasy Micro Kit (Qiagen), according to the manufacturer's instructions. The cDNA was synthesized by using iScript cDNA Synthesis Kit (Bio-Rad) starting from 1 μg of total RNA and was used as a template for qPCR analysis: reactions were performed in an iQ5 Real-Time PCR detection system (Bio-Rad) as described [4]. The rat- and mouse-specific primers were designed using Beacon Designer 2.0 software (Bio-Rad), and their sequences are listed in Online Table 1. Statistical analysis of the qPCR was performed using the iQ5 Optical System Software version 1.0 (Bio-Rad Laboratories) based on the $2^{-\Delta\Delta Ct}$ method [15]. The dissociation curve for each amplification was analyzed to confirm the absence of nonspecific PCR products.

2.8. Western blot

L6 rat myoblasts (1.0×10^6/well) were seeded in 6-well plates in DMEM with 10% FBS. After cell adhesion, cells were washed, cultured overnight at 37 °C in DMEM with 5 mM glucose, and processed for Western blot and glucose uptake experiments. For Western blot, the supernatant was removed, cells were washed once in Krebs–Ringer HEPES buffer (KRH) and then incubated in KRH with 5 mM glucose for 60 min at 37 °C with or without 100 nM ABA. The supernatant was removed, and cells were scraped in a volume of 300 μL lysis buffer (20 mM Tris–HCl pH 7.4, 150 mM NaCl, 1 mM EDTA, 1% NP40) containing a protease inhibitor cocktail. After brief sonication, the protein concentration was determined on an aliquot of each lysate. Western blot experiments were also performed on quadriceps samples isolated from wild type (WT) or LANCL2$^{-/-}$ mice, either treated or not treated with 100 nM ABA. After the explant, muscles were lysed with Tissue Lyser (Qiagen), centrifuged for 10 min at 12,000×*g*, and the supernatants were analyzed by Western blot. Lysates (70 μg proteins from tissues and 30 μg proteins from cells) were loaded on 10% polyacrylamide gel and separated by SDS-PAGE, and proteins were transferred to nitrocellulose membranes (Bio-Rad), according to standard procedures. The membranes were blocked for 1 h with 20 mM Tris–HCl pH 7.4, 150 mM NaCl, 1% Tween 20 (TBST) containing 5% non-fat dry milk and incubated for 1 h at room temperature with primary antibodies (Online Table 2). Following incubation with the appropriate secondary antibodies (Online Table 2) and ECL detection (GE Healthcare), band intensity was quantified with the ChemiDoc imaging system (Bio-Rad).

Separation of plasma membranes from whole cell lysates of L6 cells overexpressing LANCL1/2 or infected with the empty PLV vector was performed as described previously [16].

2.9. Evaluation of cell oxygen consumption

Rat L6 myoblasts infected with the empty vector PLV or overexpressing hLANCL1 or hLANCL2 were seeded at 1.5×10^6/well in a 6-well plate in complete DMEM. After 24 h, cells were incubated in DMEM without serum for 18 h, in the presence or absence of 100 nM ABA at 37 °C. At

the end of incubation, cells were recovered by trypsin treatment, resuspended at 1.5×10^6/ml in HBSS buffer, and incubated at 37 °C under continuous stirring in a 300 μL closed chamber equipped with an oxygen micro-amperometric electrode (Unisense A/S, Denmark). The rate of oxygen consumption was measured continuously for 10 min.

2.10. Glucose transport assays

Rat L6 myoblasts infected with the empty vector PLV, overexpressing hLANCL1 or hLANCL2, infected with a scramble shRNA, or silenced for the expression of both rat LANCL1 (rLANCL1) and rat LANCL2 (rLANCL2) were cultured overnight at 1.0×10^4/well in a 96-well plate in DMEM (5 mM glucose) without serum. Cells were washed once with DMEM and then incubated for 5 min at 37 °C in DMEM containing 100 nM ABA or 2 mM metformin. At the end of incubation, cells were washed with KRH at 37 °C. The fluorescently labeled deoxyglucose analog 2-NBDG (50 μM) was added to each well, and after 10 min, the supernatant was removed, wells were washed once with ice-cold KRH, 50 μL KRH was added to each well, and the mean fluorescence (λ_{ex} 465 nm, λ_{em} 540 nm) from 10 acquisitions/well was calculated. Each experimental condition was assayed in at least 8 wells. Unspecific 2-NBDG uptake, determined in the presence of the glucose transport inhibitors cytochalasin B (20 μM) and phloretin (200 μM) [8], was subtracted from each experimental value.

2.11. *In vivo* experiments

LANCL2$^{-/-}$ C57Bl/6 mice and their wild-type (WT) siblings, obtained from heterozygous breeding [5], were housed at the animal facility of the IRCCS San Martino Hospital (Genova, Italy). All protocols of animal use were approved by the Italian Ministry of Health, in line with the EU Directive 2010/63/EU for animal experiments. Seven week-old mice (9/group) fed a standard chow were administered (±)-2-cis, 4-trans abscisic acid (ABA) (Merck) at a dose of 1 μg/kg body weight (BW) in the drinking water for 4 weeks. The duration of treatment and the dose of ABA were derived from a previously published protocol [8]. The daily volume of water consumed by the animals and the average weight of the mice were preliminarily determined to calculate the ABA concentration in the drinking water necessary to yield the indicated dose. The animals were weighed weekly, and the concentration of ABA in the water was adjusted to the mean BW in each cage.

2.11.1. Oral glucose tolerance test (OGTT) in mice

One week before the end of the 4-week diet enriched with ABA or not (control), mice were fasted for 17 h before the OGTT, then 1 g/kg BW glucose was administered by gavage in 150 μL water. Blood was drawn from the tail vein before gavage (time zero) and 15, 30, 60, and 120 min after gavage: glycemia was immediately measured with a glucometer (Ascensia, Milan, Italy). Each measure was performed in duplicate.

2.11.2. Plasma ABA determination and *ex vivo* analysis of murine skeletal muscle

One week after the OGTT, the animals were sacrificed, and samples of plasma (for the determination of the ABA concentration; ELISA, Agdia) and quadriceps muscle (for qPCR and Western blot analysis) were taken and immediately frozen in liquid nitrogen.

2.12. Statistical analysis

Continuous variables are presented as mean ± SD. Comparisons were drawn by an unpaired, two-tailed Student's t-test, if not otherwise indicated. Statistical significance was set at $P < 0.05$.

3. RESULTS

3.1. Human recombinant LANCL1 binds ABA

Human recombinant LANCL1 (hLANCL1) was expressed as an N-terminal fusion protein with the enzyme glutathione S-transferase (GST). hLANCL1 was released from the GST fusion protein immobilized on glutathione-Sepharose−4B by incubation with PreScission Protease. Separately, pre-activated with DTT, in order not to expose the protein to the high DTT concentration required for activation of the PreScission Protease and similarly to the protocol used to produce hLANCL2 [16], hLANCL1 purity was checked by SDS-PAGE, revealing a single band of approximately 45 kDa, as expected (Figure 1A, left panel). hLANCL1 was eluted from a gel filtration column as a single symmetrical peak, confirming the purity of the protein (Figure 1A, right panel).

Preliminary tests were performed to assess the pH stability of the protein in anticipation of the subsequent binding experiments. To assess the stability of the recombinant protein, the fluorescent probe 8-anilinonaphthalene-1-sulfonic acid (ANS) was used. When ANS is in an aqueous solution, its excitation at 360 nm produces a low emission at about $\lambda_{em} = 545$ nm. When the dye binds to exposed hydrophobic regions of the protein, the fluorescence intensity increases, and the maximum peak emission shifts to lower wavelengths $\lambda_{em} = 460$−480. The use of this fluorophore provides information about the solvent exposure and accessibility of the hydrophobic protein domains. We performed ASN interaction experiments (Online Methods section 2.1) by incubating hLANCL1 at different pH values and in two different buffers, Na acetate and Na phosphate (Figure 1A S). These experiments showed that the ANS emission increased at pH values lower than 6, implying that the hydrophobic domains of hLANCL1 were increasingly exposed to the solvent due to protein unfolding.

Moreover, the structure of the protein was more stable in the Na acetate buffer than in the Na phosphate, in which a loss of stability had already occurred below pH 7 (Figure 1B). This behaviour was also evident in the circular dichroism (CD) experiments (Online Methods section 2.2S), in which an initial loss of the secondary structure was observed when the protein was incubated in the Na acetate buffer below pH 6. Furthermore, parallel change in the CD spectrum was observed when the protein was incubated in the Na phosphate buffer at pH values between 6 and 8, confirming reduced stability of the protein in this buffer (Figure 1C, right panel). At neutral pH, hLANCL1 showed a prevailing alpha helix secondary structure (minimum peaks at 209 and 222 nm), while at acidic pH values, the protein lost this organization and precipitated (Figure 1C).

Therefore, subsequent equilibrium binding experiments with (±)-[^{3}H]ABA were performed at pH 7.5 in Na acetate buffer. Saturable binding of (±)-[^{3}H]ABA to hLANCL1 was explored at ligand concentrations ranging from 50 nM to 5 μM (Figure 2A, left panel). Heat-denatured hLANCL1, used as the negative control, did not show any specific ABA binding (i.e., displaced by excess unlabelled ABA, not shown). The results revealed a binding curve with a single K_d in the low micromolar range (1.0 ± 0.4 μM), a value lying in between the K_d values of the high- and the low-affinity binding sites previously discovered in hLANCL2 [17], and a B_{max} of 254 pmol/mg protein. Equilibrium binding experiments were performed both in the presence and absence of 1.0 mM GSH, and no significant difference in the affinity constant was observed.

SPR experiments of hLANCL1 with or without (±)-ABA were performed at pH 5.8 to compromise between an acidic pH, yielding the highest binding of the protein to the chip and a value compatible with a conserved protein structure (Figure 2A S). Based on the results

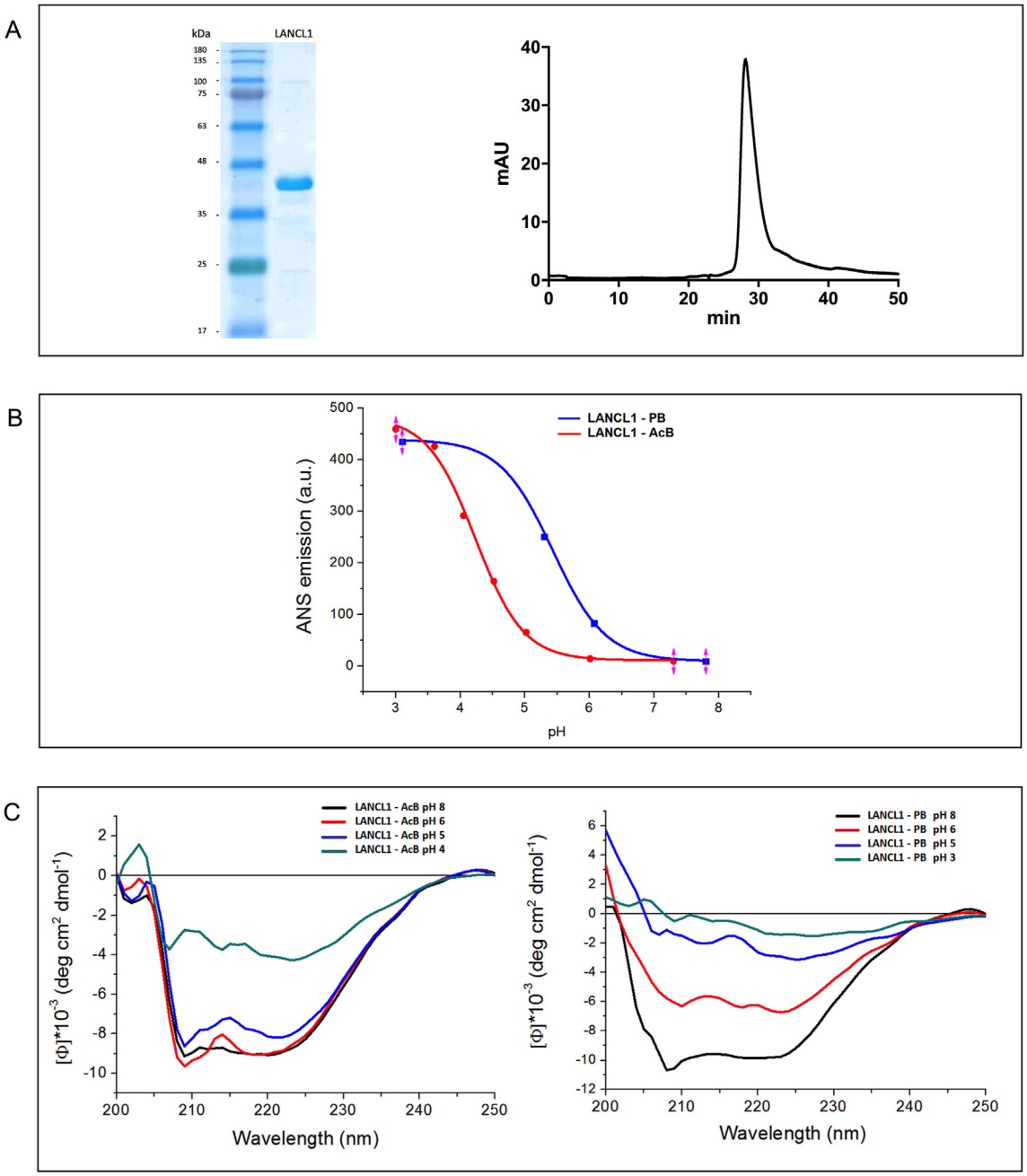

Figure 1: Characterization of human recombinant LANCL1. A. Determination of recombinant hLANCL1 protein purity; *left panel*, representative SDS—PAGE of 5 μg purified hLANCL1 used in the binding experiments; the gel was stained with ProSieve Blue Protein Staining solution; hLANCL1 migrated as a single band with an apparent molecular mass of 45 kDa; *right panel*: size exclusion chromatography of purified hLANCL1 on a TSK-gel 3000SWXL column revealed a single symmetrical peak. **B.** Binding of 8-Anilinonaphthalene 1-Sulfonic Acid (ANS) to recombinant hLANCL1; representative fluorescence emission spectrum of ASN incubated with hLANCL1 at different pH values. The effect of pH on LANCL1 unfolding was evaluated by monitoring the ANS emission in Na acetate (AcB) or in Na phosphate (PB) buffer. The concentration of LANCL1 in Na acetate and Na phosphate was 6.4 μM and 5.4 μM, respectively. **C.** Circular dichroism (CD) spectroscopy; representative CD spectra of recombinant hLANCL1 incubated in AcB, *left panel*, and PB, *right panel*, at different pH values.

obtained by CD on the folding state of hLANCL1 in the Na acetate buffer at various pH values (Figure 1C), the covalent coupling ability of the protein to the SPR CM7 chip was evaluated in a range of pH values compatible with protein stability (10 mM Na acetate buffer pH 5.5, 5.8, 6.0, 6.5 at a constant protein concentration of 30 μg/ml) to determine the best conditions for achieving the highest pre-concentration possible. The results suggested performing the covalent amine coupling of hLANCL1 to the carboxymethyl groups of the sensor chip in 10 mM Na acetate, pH 5.8 (Figure 2A S). The total amount of hLANCL1 immobilised was 36980 resonance units (RUs). The binding of ABA to hLANCL1 was performed by injecting ABA dissolved at a micromolar concentration range. SPR analysis revealed the presence of an ABA binding site with an affinity constant of 11.5 ± 3.1 μM (Figure 2A, right panel).

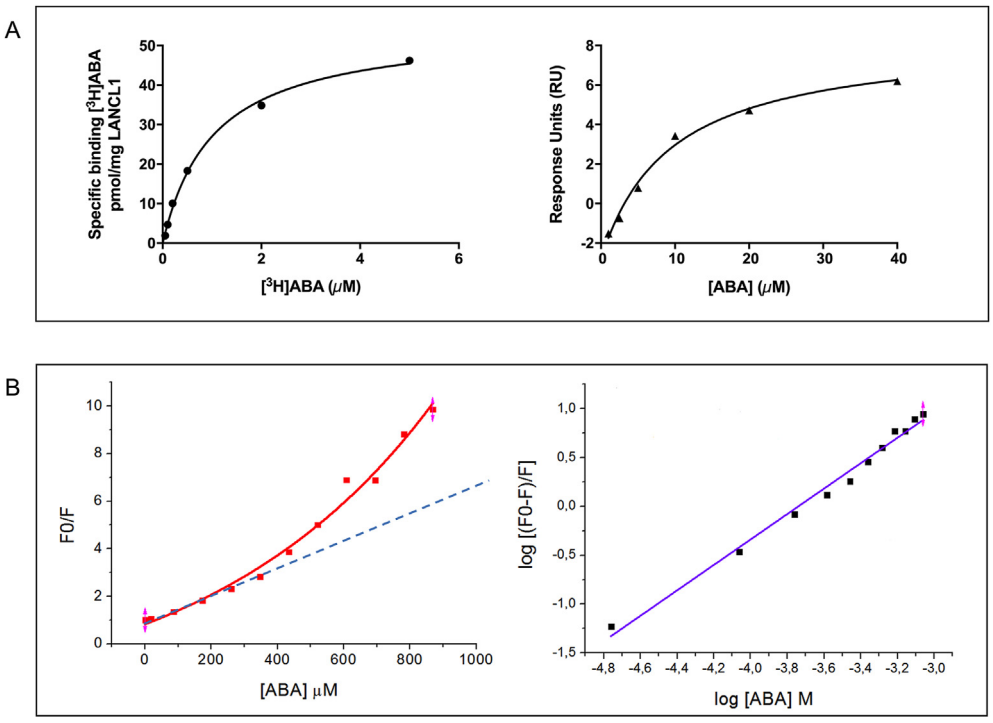

Figure 2: Recombinant hLANCL1 binds ABA. A. [^{3}H]ABA equilibrium binding (*left panel*). Saturation binding experiments were performed as described in Section 2.3. Human purified LANCL1 was incubated with 50 nM (±)-[^{3}H]ABA in the presence of increasing concentrations of unlabeled ABA. The specific binding was analyzed by nonlinear regression, using the GraphPad Prism software. Results are the mean ± SD of 6 experiments. Surface plasmon resonance (SPR) (*right panel*). hLANCL1 was immobilized by amine coupling on a CM7 chip in 10 mM Na acetate pH 5.8. The steady-state K_d value (11.5 μM) was estimated using the Biacore T200 evaluation software. The values shown are the mean ± SD from 3 experiments. B. Fluorescence quenching emission analysis of the interaction between ABA and recombinant hLANCL1. *Left panel*, dynamic quenching. LANCL1 (8.65 μM) was incubated with increasing concentrations of ABA to obtain a molar ratio LANCL1/ABA ranging from 1:2 to 1:450. All emission spectra were recorded on a luminescence spectrometer at excitation wavelengths of 280 nm (slit width = 5 nm). The dynamic quenching constants were determined using the equation: $F_0/F = 1+K_{SV}[Q]$, where F_0 and F are the fluorescence intensities of hLANCL1 without and with ABA, respectively, [Q] is the concentration of ABA, and KSV is the Stern–Volmer quenching constant. *Right panel*, static quenching. The static quenching constant, or binding constant, K_a, and the number of ABA-binding sites, n, were calculated using the equation: $\log[(F_0-F)/F] = \log K_a + n \log[Q]$.

To further confirm ABA binding to hLANCL1, a fluorescence analysis based on the emission spectra of tryptophan residues at 335 nm was used. When the tryptophan residues of the hLANCL1 protein were selectively excited by irradiating at 280 nm, the emission spectrum showed a maximum at 335 nm, indicating that the tryptophan residues are buried inside the hydrophobic core of the protein [18]. When ABA was added to LANCL1 in the solution to obtain a molar ratio between LANCL1 and ABA ranging from 1:2 to 1:450, the intensity of the spectra decreased (Figure 2B S), indicating that ABA was able to quench the tryptophan emission of hLANCL1. Two common mechanisms for fluorescence quenching are dynamic and static quenching. To determine which was taking place, the linearity of the Stern–Volmer plot was interpreted, as previously described [13]. The Stern–Volmer plot of F_0/F, where F_0 and F corresponded to the fluorescence intensities of hLANCL1 without and with ABA, respectively, relative to the ABA concentration, results in an exponential curve, which is typical of proteins that have tryptophan residues in different environments (e.g., buried residues versus residues exposed on the surface) (Figure 2B, left panel). For static quenching, the binding constant (K_a) for the formation of an adduct between the hLANCL1 and ABA was determined using a double logarithmic plot. The binding site values (n) were also determined from the slope using the following equation: $\log[(F_0-F)/F] = \log K_a + n\log[ABA]$. The calculated K_a value for LANCL1 and ABA was 2.3×10^4, for a K_d of 4.3 μM (Figure 2B, right panel).

Taken together, results obtained with three different techniques allow us to conclude that hLANCL1 binds to ABA with a constant affinity in the low micromolar range (1.0 μM, by equilibrium binding, 4.3 μM by fluorescence quenching analysis, and 11.5 μM by SPR). The higher K_d calculated with the SPR may be due to the acidic pH required to optimize the protein binding to the chip (pH 5.8), a pH which lies close to values denaturing the native protein structure, as observed by ANS analysis and CD experiments (Figure 1B,C), possibly unmasking low-affinity sites also present in LANCL2 with a similar K_d value (approx. 18 μM) [17].

3.2. LANCL1 overexpression increases glucose transport *via* GLUT4 in L6 myoblasts

As LANCL2 has been reported to stimulate glucose transport in muscle cells *via* an insulin-independent increase of GLUT4 expression [8], we investigated a possible role of LANCL1 in the same function. To this end, we undertook the stable silencing of both rLANCL1 and rLANCL2 and the overexpression of either of the proteins in rat L6 myoblasts. Silencing both proteins was achieved by the lentiviral infection of L6 with hLANCL1-and hLANCL2-specific shRNAs. After puromycin selection of the infected cells, knockdown of both LANCL1 and LANCL2 was confirmed by both qPCR (Figure 3A, central panel) and immunoblot (Figure 3A, right panel). Overexpression of LANCL1 and LANCL2 was obtained by retroviral infection and was confirmed by immunoblot (Figure 3A, left panel). If not otherwise indicated, all experiments were

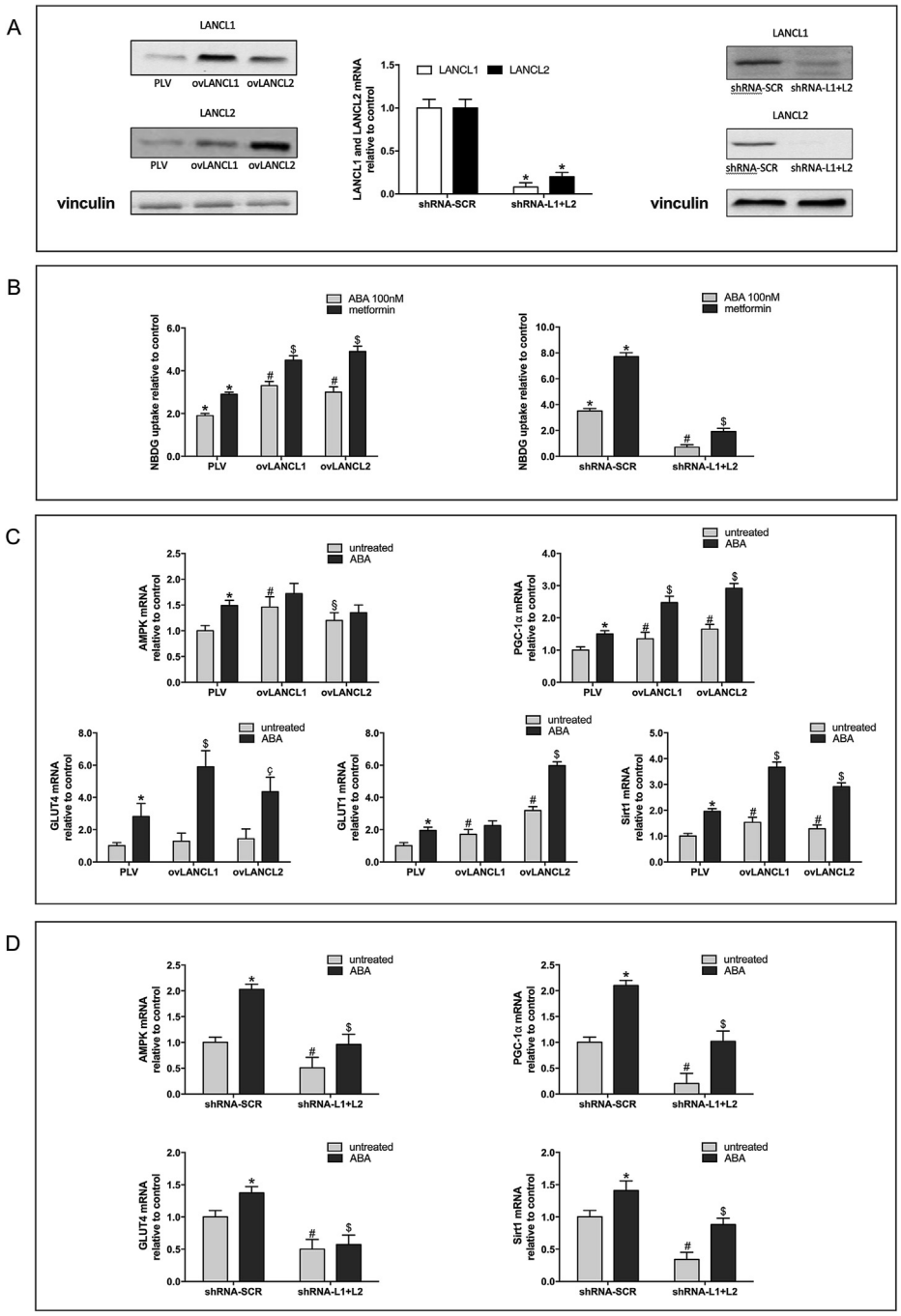

Figure 3: LANCL1 and LANCL2 control ABA-sensitive glucose uptake in L6 myoblasts by regulating transcription of GLUT4/GLUT1 *via* the AMPK/PGC-1α/Sirt1 pathway. A. LANCL1 and LANCL2 were stably overexpressed or silenced in rat L6 myoblasts by viral infection; *left panel*, representative Western blot of LANCL1/2 proteins in cells overexpressing LANCL1 (ovLANCL1) or LANCL2 (ovLANCL2); *right panel*, representative Western blot of LANCL1/2 proteins in cells silenced for both proteins (shRNA-L1+L2); *central panel*, LANCL1/2 mRNA levels relative to control in LANCL1/2- silenced cells, mean ± SD values from 3 different determinations. $*p < 0.0002$ by unpaired two-tailed t-test compared with control cells, infected with the scramble shRNAs (shRNA-SCR). If not otherwise indicated, in all subsequent experiments ovLANCL1 and ovLANCL2 cells showed an approx. 4- and 6-fold higher expression of LANCL1 and LANCL2, respectively, as compared with PLV. Cells silenced for the expression of LANCL1 and LANCL2 showed an 80% reduction of the expression of LANCL1 and LANCL2 as compared to control cells infected with shRNA-SCR. **B.** L6 cells overexpressing LANCL1 (ovLANCL1) or LANCL2 (ovLANCL2) or silenced for the expression of both proteins (shRNA-L1+L2) were serum-starved for 12 h, then treated with 100 nM ABA or with 2 mM metformin for 5 min prior to incubation with the fluorescent glucose analog NBDG. *Left panel*, NBDG uptake in overexpressing cells, relative to control, untreated cells, infected with the empty vector (PLV); $^{*}p < 0.0004$ relative to untreated PLV; $^{\#}p < 0.001$ relative to ABA-treated PLV; $^{\$}p < 0.0002$ relative to metformin-treated PLV; *right panel*, NBDG uptake in silenced cells, relative to control, untreated cells, infected with the scramble (SCR) shRNA; $^{*}p < 0.00004$ relative to untreated shRNA-SCR-infected cells; $^{\#}p < 0.00007$ relative to ABA-treated shRNA-SCR-infected cells; $^{\$}p < 0.00001$ relative to metformin-treated shRNA-SCR-infected cells. All results are the mean ± SD from at least 3 separate experiments. **C-D.** The same cells as shown in B were serum-starved for 12 h, then treated with 100 nM ABA for 4 h mRNA levels of the indicated proteins are expressed relative to untreated control cells, infected with the empty vector (PLV) (panel C), or with the scramble shRNAs (panel D). Results are the mean ± SD from 3 separate experiments; $^{*}p < 0.02$ relative to untreated control cells, $^{\#}p < 0.05$ and $^{\S}p < 0.05$ relative to untreated control; $^{\$}p < 0.01$ and $^{\text{¢}}p < 0.02$ relative to ABA-treated control. P values are calculated by unpaired, two-tailed t-test.

performed with a silencing efficiency of approx. 80% for both LANCL1 and LANCL2 relative to control cells infected with a scramble shRNA and an overexpression of approx. 4-fold for LANCL1 and 6-fold for LANCL2 relative to control cells infected with an empty PLV vector.
In L6 infected with the empty vector (PLV), ABA stimulated NBDG uptake approx. 2-fold compared to untreated controls. Overexpression of either LANCL1 or LANCL2 increased the ABA-induced stimulation of NBDG uptake (Figure 3B, left panel) and increased the effect of metformin, a stimulator of cell glucose uptake *via* GLUT4 [19]. Conversely, silencing both LANCL1 and LANCL2 had the opposite effect, abrogating the effect of ABA on NBDG uptake and significantly reducing the metformin (Figure 3B, right panel), indicating that ABA and metformin share the same effector kinase AMPK.
Indeed, the stimulation of glucose transport by ABA *via* LANCL2 occurs by the activation of AMPK and increased transcription of PGC-1α [8]; thus, we compared the effect of the overexpression of either LANCL2 or LANCL1 on the transcription of AMPK and PGC-1α in L6 myoblasts. In LANCL2-overexpressing cells as compared to cells infected with the empty vector, an increased transcription of AMPK, PGC-1α, and Sirtuin 1 (Sirt1), all key players in muscle function and metabolism [20], was observed, together with an increased GLUT4 transcription (Figure 3C). Interestingly, GLUT1-specific mRNA was also more abundant in LANCL2-overexpressing cells. Treatment with 100 nM ABA for 4 h further increased the transcription of all proteins (Figure 3C). A similar pattern of results was observed on LANCL1-overexpressing cells, indicating that AMPK, PGC-1α, Sirt1, GLUT4, and GLUT1 are also targets of LANCL1 (Figure 3C).

3.3. LANCL1 and LANCL2 control the expression of AMPK, GLUT4, PGC-1α, and Sirt1

The fact that LANCL1-or LANCL2-overexpression *per se*, i.e., without the addition of ABA, increased transcription of AMPK, GLUT4, GLUT1, PGC-1α and Sirt1 suggested to investigate the effect of LANCL1/2 silencing the transcription of the same regulatory proteins. Indeed, the combined silencing of LANCL1 and LANCL2 significantly reduced the basal (unstimulated) level of mRNAs for all the regulatory proteins and GLUT4 compared to control cells infected with scramble-shRNAs (Figure 3D). Upon incubation with 100 nM ABA for 4 h, the levels of all mRNAs explored increased in LANCL1/2-silenced cells, except for the GLUT4 mRNA, though they remained below those measured in untreated, scramble-silenced cells (Figure 3D). The partial abrogation of the response to ABA may be attributed to the incomplete knockdown of LANCL1/2 expression accomplished by shRNA infection (approx. 80%). Taken together, the observations of increases in the overexpression of either LANCL1 or LANCL2 and that silencing LANCL1/2 reduces the transcription of AMPK, PGC-1α, Sirt1, and GLUT4, indicate a transcriptional control by LANCL1/2 on these genes.
At the protein level, the total AMPK increased slightly in L6 cells overexpressing LANCL2, but not LANCL1; upon treatment with ABA, both AMPK (Figure 4A, upper left panel) and pAMPK (Figure 4A, upper right panel) significantly increased in cells overexpressing either LANCL1 or LANCL2, indicating that both LANCL1 and LANCL2 stimulate AMPK protein expression and phosphorylation upon ABA binding. A higher amount of the total and phosphorylated AMPK increases the enzymatic activity of the kinase, both potential and actual, on its different substrates. Thus, although the pAMPK/AMPK ratio was similar in control and in LANCL1/2-overexpressing cells incubated with ABA, the significantly higher total amounts of pAMPK and AMPK in the overexpressing cells implies a higher kinase activity. PGC-1α, GLUT1, and GLUT4 protein expression increased in both LANCL1-and LANCL2-overexpressing L6 cells approx. 2-fold compared to control cells, and treatment with ABA further increased PGC-1α, GLUT1, and GLUT4 protein levels (Figure 4A, lower panel). Thus, upon ABA treatment, L6 cells overexpressing either LANCL1 or LANCL2 respond similarly with an increase of total and phosphorylated AMPK, PGC-1α, GLUT1, and GLUT4, confirming the protein level results obtained by qPCR.
Silencing both LANCL1 and LANCL2 resulted in a significant reduction of total and phosphorylated AMPK, which increased slightly upon ABA treatment of the cells but remained lower than in control cells infected with scramble-shRNAs (Figure 4B, upper right and left panels). PGC-1α, GLUT1, and GLUT4 protein levels were lower in double-silenced cells as compared to that in control cells and remained below the levels of control cells upon treatment with ABA (Figure 4B, lower panel).
Finally, GLUT4 and GLUT1 proteins increased significantly in the plasmamembrane-enriched fractions from both LANCL1-and LANCL2-overexpressing L6 cells compared to control PLV-infected cells (approx. 4-fold for GLUT1 and 2-fold for GLUT4; Figure 4C). Treatment with ABA further significantly increased the plasmamembrane translocation of both glucose transporters in LANCL1/2-overexpressing cells (approx. 8-fold for GLUT1 and 4-fold for GLUT4, relative to control cells).
Together, the results obtained on LANCL1/2-overexpressing or -silenced L6 cells suggest that both LANCL proteins transduce an ABA-triggered response, activating AMPK transcription and phosphorylation, increased expression of the transcription factor PGC-1α, and higher levels of GLUT4 and GLUT1 transcription, protein expression, and translocation to the plasmamembrane.

3.4. LANCL1 and LANCL2 control mitochondrial DNA content and expression of uncoupling proteins sarcolipin and UCP3 in L6 cells

ABA treatment has been previously shown to increase the expression of browning genes *in vitro*, in murine preadipocytes, and *in vivo*, in the BAT from ABA-treated mice [11]. Overexpression of LANCL1, but not of LANCL2, increased the expression of the SM-specific uncoupling protein sarcolipin; upon treatment with ABA, both LANCL1-and LANCL2-overexpressing cells showed a significantly increased sarcolipin expression, higher than that observed in control cells treated with ABA (Figure 5A, upper left panel). Silencing both LANCL1 and LANCL2 significantly reduced sarcolipin expression and abrogated the effect of ABA (Figure 5A, lower left panel), indicating that both LANCL proteins control the expression of sarcolipin. Total mitochondrial DNA, a measure of a mitochondrial number, did not increase in LANCL1-or LANCL2-overexpressing cells (Figure 5A, upper central panel); however, the combined silencing of both proteins significantly reduced mitochondrial DNA content in L6 cells compared to control cells (Figure 5A, lower central panel). These results indicate that the basal L6 cell expression of LANCL1/2 is both required and sufficient for the maintenance of mitochondrial DNA levels. Expression of UCP3, the most abundantly expressed member of the UCP family in the SM [21], was also investigated. UCP3 mRNA increased approx. 10-fold in LANCL1-overexpressing L6 compared to control cells; a significant (approx. 5-fold) increase of UCP3 mRNA was also observed in LANCL2-overexpressing cells (Figure 5A, upper right panel). Silencing both LANCL1 and LANCL2 drastically reduced the transcription of UCP3 mRNA compared to control cells and significantly reduced the response to the stimulatory effect of ABA on UCP3 transcription (Figure 5A, lower right panel). Conversely, the expression of UCP1, both at the mRNA (Figure 3A S) and protein level (Figure 3B S), was only slightly increased in LANCL1/2-overexpressing cells.
Finally, cell respiration was evaluated: in L6 cells overexpressing either LANCL1 or LANCL2 O_2 consumption increased significantly compared

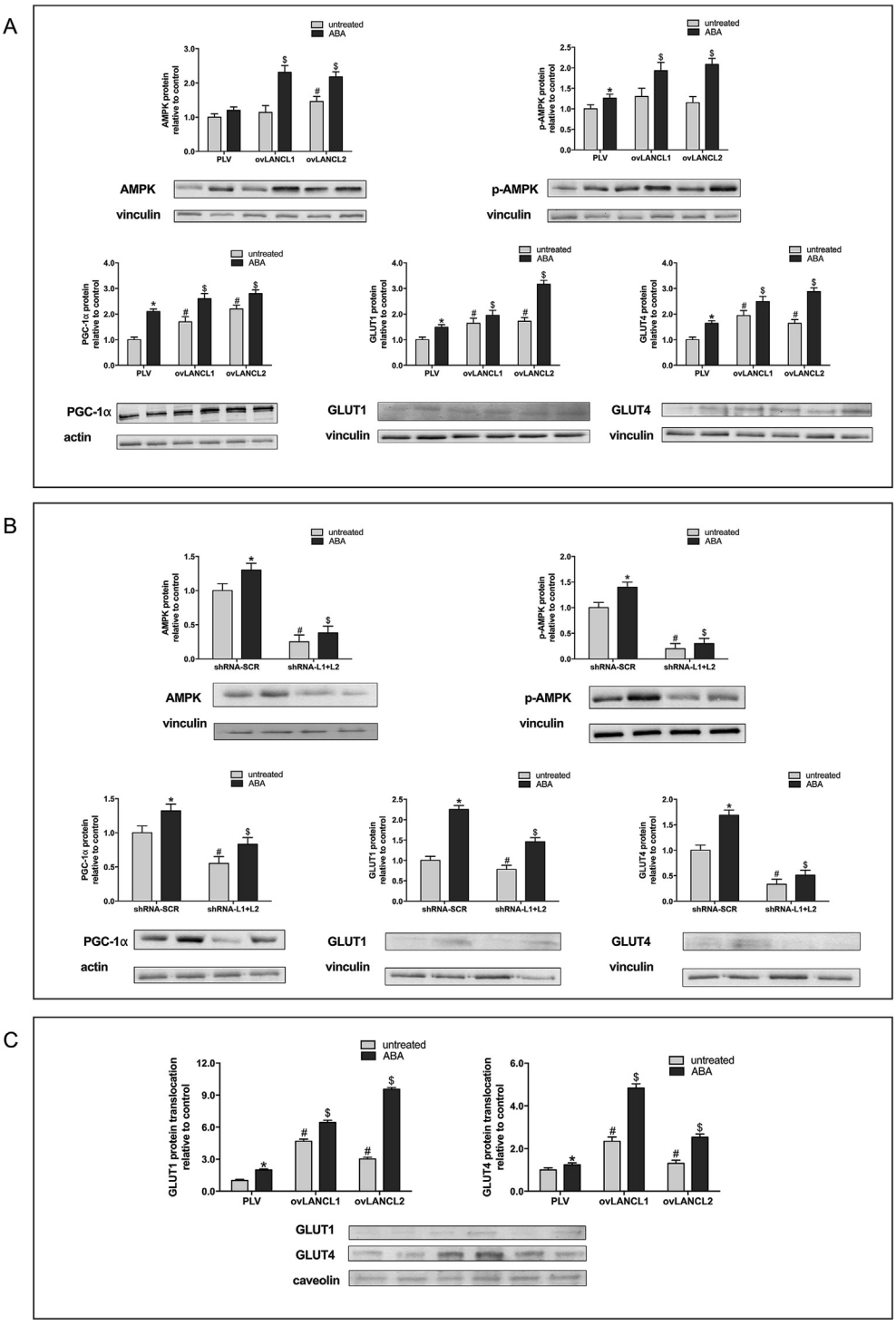

Figure 4: LANCL1 and LANCL2 regulate ABA-sensitive AMPK, pAMPK, and PGC-1α protein levels in L6 myoblasts. The same cells as shown in Figure 3A, serum-starved for 12 h and then incubated without or with 100 nM ABA for 1 h, were also analyzed by Western blot for expression of the indicated proteins. **A.** *Upper left panel*, total AMPK in cells overexpressing LANCL1 (ovLANCL1) or LANCL2 (ovLANCL2), relative to control cells, infected with the empty vector and untreated (PLV). *Upper right panel*, phosphorylated (Ser473) AMPK (pAMPK) relative to PLV. *Lower left panel*, PGC-1α relative to PLV. *Lower central panel*, GLUT1 relative to PLV. *Lower right panel*, GLUT4 relative to PLV. $^{*}p < 0.03$ relative to untreated control, $^{\#}p < 0.006$ relative to untreated control; $^{\$}p < 0.02$ relative to ABA-treated PLV-infected cells. **B.** *Upper left panel*, total AMPK in cells silenced for LANCL1 and LANCL2 expression (shRNA-L1+L2) relative to control cells, infected with the scramble shRNAs and untreated (shRNA-SCR). *Upper right panel*, phosphorylated (Ser473) AMPK (pAMPK) relative to shRNA-SCR. *Lower left panel*, PGC-1α relative to shRNA-SCR. *Lower central panel*, GLUT1 relative to shRNA-SCR. *Lower right panel*, GLUT4 relative to shRNA-SCR. $^{*}p < 0.02$ relative to untreated control, $^{\#}p < 0.01$ relative to untreated control; $^{\$}p < 0.008$ relative to ABA-treated shRNA-SCR-infected cells. **C.** Plasmamembrane-enriched lysates from LANCL1/2-overexpressing L6 cells treated or not with ABA have been obtained as described in Section 2.8. *Left panel*, GLUT1 relative to PLV. *Right panel*, GLUT4 relative to PLV. $^{*}p < 0.04$ relative to untreated control, $^{\#}p < 0.008$ relative to untreated control; $^{\$}p < 0.03$ relative to ABA-treated PLV-infected cells. Each panel shows the mean ± SD of at least 3 separate experiments and a representative Western blot for each protein investigated. P values are calculated by unpaired two-tailed t-test.

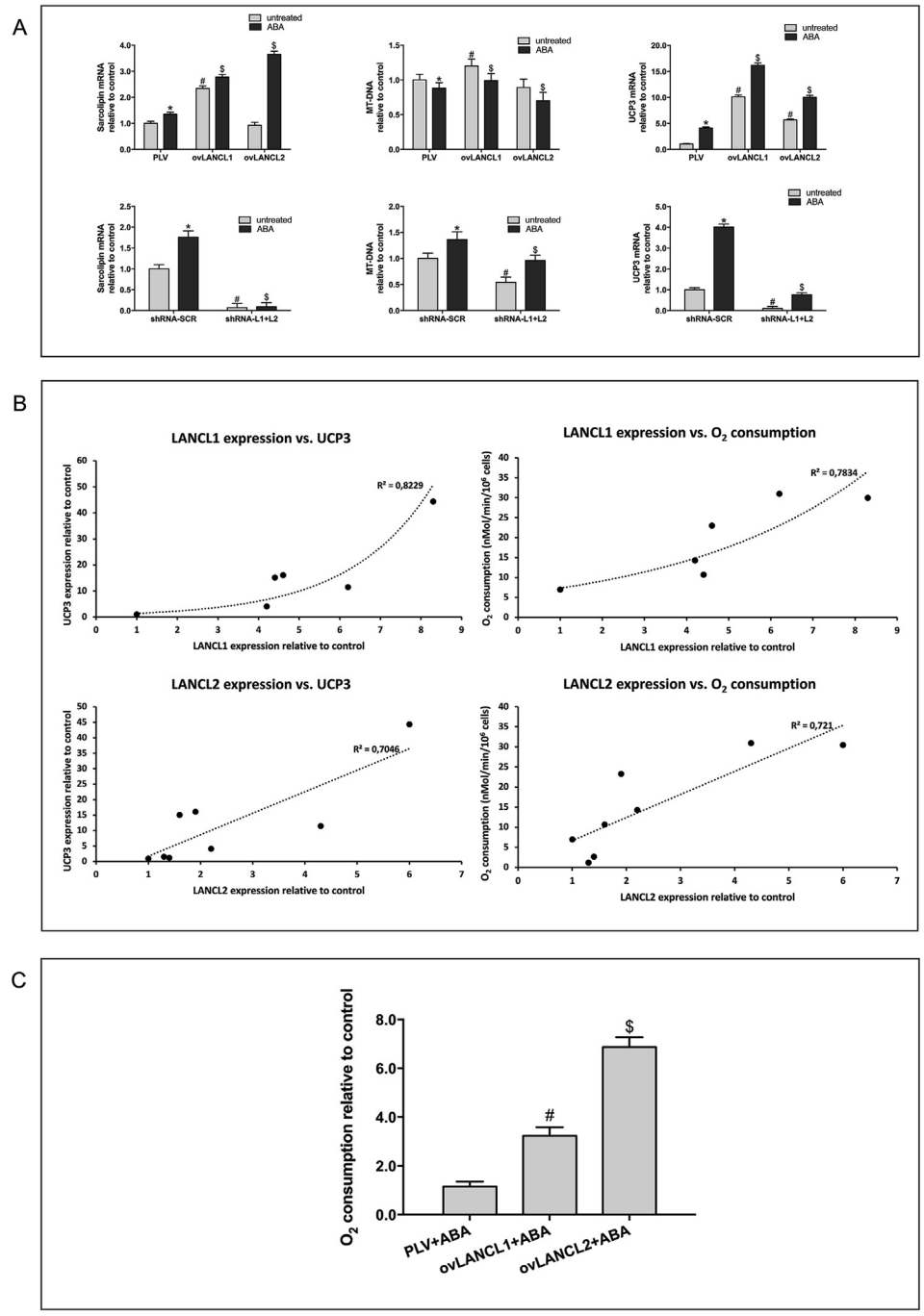

Figure 5: LANCL1 and LANCL2 control expression levels of the uncoupling proteins sarcolipin and UCP3 and stimulate ABA-sensitive mitochondrial respiration in L6 cells. L6 myoblasts overexpressing LANCL1 (ovLANCL1) or LANCL2 (ovLANCL2) or silenced for the expression of both proteins (shRNA-L1+L2) were serum-starved for 12 h and then incubated without or with 100 nM ABA for 4 h. **A**. *Upper left panel*, sarcolipin mRNA, *upper central panel,* mitochondrial DNA (MT-DNA), *upper right panel*, UCP3 mRNA in LANCL1/2 overexpressing cells relative to control cells, infected with the empty vector and untreated (PLV); $^{*}p < 0.008$ relative to untreated PLV-infected cells, $^{\#}p < 0.05$ relative to untreated control, $^{\$}p < 0.03$ relative to ABA-treated PLV-infected cells. *Lower left panel*, sarcolipin mRNA, *lower central panel*, mitochondrial DNA (MT-DNA), *lower right panel*, UCP3 mRNA in cells silenced for LANCL1 and LANCL2, relative to control cells, infected with the scramble shRNAs and untreated (shRNA-SCR). $^{*}p < 0.02$ relative to untreated control, $^{\#}p < 0.005$ relative to untreated control; $^{\$}p < 0.02$ relative to ABA-treated shRNA-SCR-infected cells. Each panel shows the mean ± SD of at least 3 separate experiments. P values are calculated by unpaired two-tailed t-test. **B.** Correlation between the expression level of LANCL1 (*upper panels*) or of LANCL2 (*lower panels*) in ovLANCL1 or ovLANCL2 cells and UCP3 mRNA (*left panels*) or cell O_2 consumption (*right panels*). LANCL1/2 and UCP3 mRNA levels are relative to the respective mRNA in cells infected with the empty vector (control). O_2 consumption is expressed in nMoles/min/10^6 cells. Each point is the mean of at least two separate determinations, performed on cells at different time points after infection and antibiotic selection. The value of R^2 of the best-fitting curve is shown. **C**. O_2 consumption by L6 myoblasts overexpressing LANCL1 (ovLANCL1) or LANCL2 (ovLANCL2), approx. 4- and 6-fold relative to cells infected with the empty vector (PLV). Cells were incubated for 18 h at 37 °C in DMEM in the presence or absence of 100 nM ABA. Oxygen consumption was measured in a cell suspension with a micro-amperometric electrode. The panel shows the rate of oxygen consumption of ABA-treated cells relative to control cells not treated with ABA. $^{\#}p < 0.0009$ relative to ABA-treated PLV-infected cells; $^{\$}p < 0.00002$ relative to ABA-treated PLV-infected cells. Data are means ± SD of three different experiments.

to control cells, and the preincubation of cells with 100 nM ABA for 12 h further stimulated respiration, which is significantly more in the overexpressing cells compared to cells infected with the empty vector (Figure 5C). Expression levels of both LANCL1 and LANCL2, which increased over several weeks of the culture of the cells, correlated with UCP3 mRNA levels and with cell respiration. The correlation between the LANCL1 expression and UCP3 mRNA levels (Pearson $R = 0.906$; $p = 0.013$), or O_2 consumption (Pearson $R = 0.886$; $p = 0.019$), was best described by an exponential curve, whereas the correlation between LANCL2 expression and UCP3 mRNA (Pearson $R = 0.839$; $p = 0.009$), or O_2 consumption (Pearson $R = 0.849$; $p = 0.008$), was best described by a line. When the expression levels of both LANCL1 and LANCL2 were plotted against UCP3 mRNA levels (Pearson $R = 0.837$; $p = 0.0004$), or cell O_2 consumption (Pearson $R = 0.802$; $p = 0.0006$), a linear correlation was observed. Together, these results suggest that both LANCL1 and LANCL2 control the expression of UCP3 and cell respiration rate, with LANCL1 transcription levels correlating with a logarithmic increase in UCP3 expression and cell respiration.

Indeed, silencing both LANCL1 and LANCL2 greatly reduced the expression of PGC-1α (Figure 3D, upper right panel), a master regulator of mitochondrial function [22]. Interestingly, silencing both LANCL1 and LANCL2 also greatly reduced (by approx. 75%) the expression of Sirt1 (Figure 3D, lower right panel), another key regulator (along with AMPK and PGC-1α) of skeletal muscle metabolism and function [20].

3.5. ABA improves glucose tolerance in LANCL2$^{-/-}$ mice by stimulating muscle GLUT4 expression *via* the LANCL1/AMPK/PGC-1α pathway

A normal fasting glycemia but a significantly reduced glucose tolerance had been previously observed in male LANCL2$^{-/-}$ mice [5] and was confirmed by comparing the glycemia profile of wild-type (WT) and LANCL2$^{-/-}$ mice after an oral glucose load (Figure 6A, left panel). Within a 0–30 min time frame, glycemia increased significantly faster in LANCL2$^{-/-}$ mice than WT mice (3.7 ± 1.3 *vs.* 2.3 ± 0.9 mg/dL/min, $p = 0.001$). Both WT and LANCL2$^{-/-}$ mice responded to chronic ABA treatment (1 μg/kg BW/day for 4 weeks) with a significant reduction of the area-under-the-curve (AUC) of glycemia (Figure 6A, right panel), indicating that the absence of LANCL2 did not abrogate sensitivity to the glycemia-lowering action of ABA. Therefore, the expression levels of LANCL1 in the SM from LANCL2$^{-/-}$ and WT mice were compared.

SM expression of LANCL1 was significantly higher in quadriceps muscles from LANCL2$^{-/-}$ mice compared to WT controls, and chronic treatment of the animals with oral ABA further increased LANCL1 expression, at both the protein (Figure 6B, left panel) and mRNA levels (Figure 6B, right panel). LANCL1 and LANCL2 controlled levels of AMPK/PGC-1α/Sirt1 and GLUT4/1 in L6 cells (Figures 3, 4); thus, we compared the expression of these proteins in SM biopsies from WT and LANCL2$^{-/-}$ mice, treated with ABA or not. Chronic ABA treatment significantly increased muscle expression of AMPK, PGC-1α, and GLUT4 in the SM from WT mice. SM from LANCL2$^{-/-}$ mice showed higher protein levels of PGC-1α and GLUT4 than WT controls, which did not further increase upon ABA treatment (excluding AMPK) and were similar to those of WT mice treated with ABA (Figure 6C, left panel). The ratio between pAMPK and AMPK protein levels in ABA-treated and −untreated mice, both WT and KO, was similar and approximately 1 (not shown), in line with what was observed in L6 cells overexpressing LANCL1 or LANCL2.

mRNA levels of AMPK, PGC-1α, GLUT4, and GLUT1 were all significantly higher in the SM from WT and LANCL2$^{-/-}$ mice treated with ABA compared to the respective untreated controls (Figure 6C, right panel), and the extent of increase was similar in WT and LANCL2$^{-/-}$ mice, indicating that the genetic ablation of LANCL2 does not affect the stimulatory effect of oral ABA on the transcription of those proteins. Finally, chronic ABA treatment significantly increased the transcription of Sirt1 and NAMPT in the SM from both WT and LANCL2$^{-/-}$ mice (Figure 6C). NAMPT overexpression in SM has been reported to promote cell survival (by maintaining mitochondrial NAD^+ levels [23]) and to increase mitochondrial gene expression and ameliorate exercise endurance in mice [24]. Indeed, we observed an increased physical endurance in mice chronically treated with low-dose ABA [8]. Interestingly, increased transcription of both Sirt1 and NAMPT was observed as early as 30–60 min after the addition of 100 nM ABA to muscle biopsies from WT mice *ex vivo* (Figure 4 S), indicating that the transcriptional stimulation by ABA on these target proteins is fast and direct (i.e., occurring without the intervention of blood-borne signaling molecules).

Sarcolipin and mitochondrial DNA content were affected by LANCL1/2 expression levels and by ABA in L6 myoblasts (Figure 5A,B); in the SM from ABA-treated WT and LANCL2$^{-/-}$, mice sarcolipin increased significantly (approx. 5-fold) and similarly to the respective ABA-untreated controls (Figure 6D, left panel). The mitochondrial DNA content in the SM from ABA-treated WT mice also increased compared to untreated controls (approx. 2-fold), whereas LANCL2$^{-/-}$ mice had (basal) higher levels of mitochondrial DNA compared to WT animals, possibly the result of higher LANCL1 expression levels (Figure 6B), which further slightly (and not significantly) increased upon treatment with ABA (Figure 6D, central panel). These results confirm the role of ABA in increasing the SM expression of sarcolipin and mitochondrial DNA content *in vivo* and indicate that LANCL2 is not essential in mediating this effect.

UCP3 was highly expressed in the SM from ABA-treated WT mice compared to untreated controls (approx. 9-fold). SM from LANCL2$^{-/-}$ mice showed a 2-fold higher expression of UCP3 compared to SM from WT mice and also responded to ABA with a further significant increase of UCP3 expression, similar to that observed in ABA-treated WT mice (Figure 6D, right panel).

4. DISCUSSION

One of the established features of LANCL2 is to behave as an ABA receptor, allowing the hormone's functional effects to take place in ABA-responsive cells [4,25]. Here we show that LANCL1 also binds ABA with a calculated K_d in the low micromolar, a value which lies in between those of the high- and low-affinity binding sites of LANCL2 for ABA (0.1 and 10 μM, respectively [17]). The lower affinity for the ABA of LANCL1 compared to LANCL2 may be responsible for the impairment of glucose tolerance observed in LANCL2$^{-/-}$ mice in both males (Figure 6A left panel) and females (Online Figure 5). LANCL2$^{-/-}$ mice showed a higher glycemia AUC after glucose load than WT siblings, despite an increased expression of LANCL1 in the SM (Figure 6B). It may be hypothesized that glucose tolerance would have been worse in LANCL2$^{-/-}$ mice if LANCL1 were not concomitantly overexpressed in the SM. However, exogenous ABA administration resulting in an approximately 1-log higher plasma ABA concentration in ABA-treated vs. −untreated mice (not shown) improves glucose tolerance in LANCL2$^{-/-}$ mice (Figure 6A, right panel). This result suggests that an increase of ABAp, obtained by administering a daily dose of 1 μg/kg BW, elicits a fully functional response by LANCL1. A 10-fold increase of ABAp can occur after consuming large amounts of ABA-rich food or vegetal extracts containing ABA [26]. Interestingly, ABA treatment

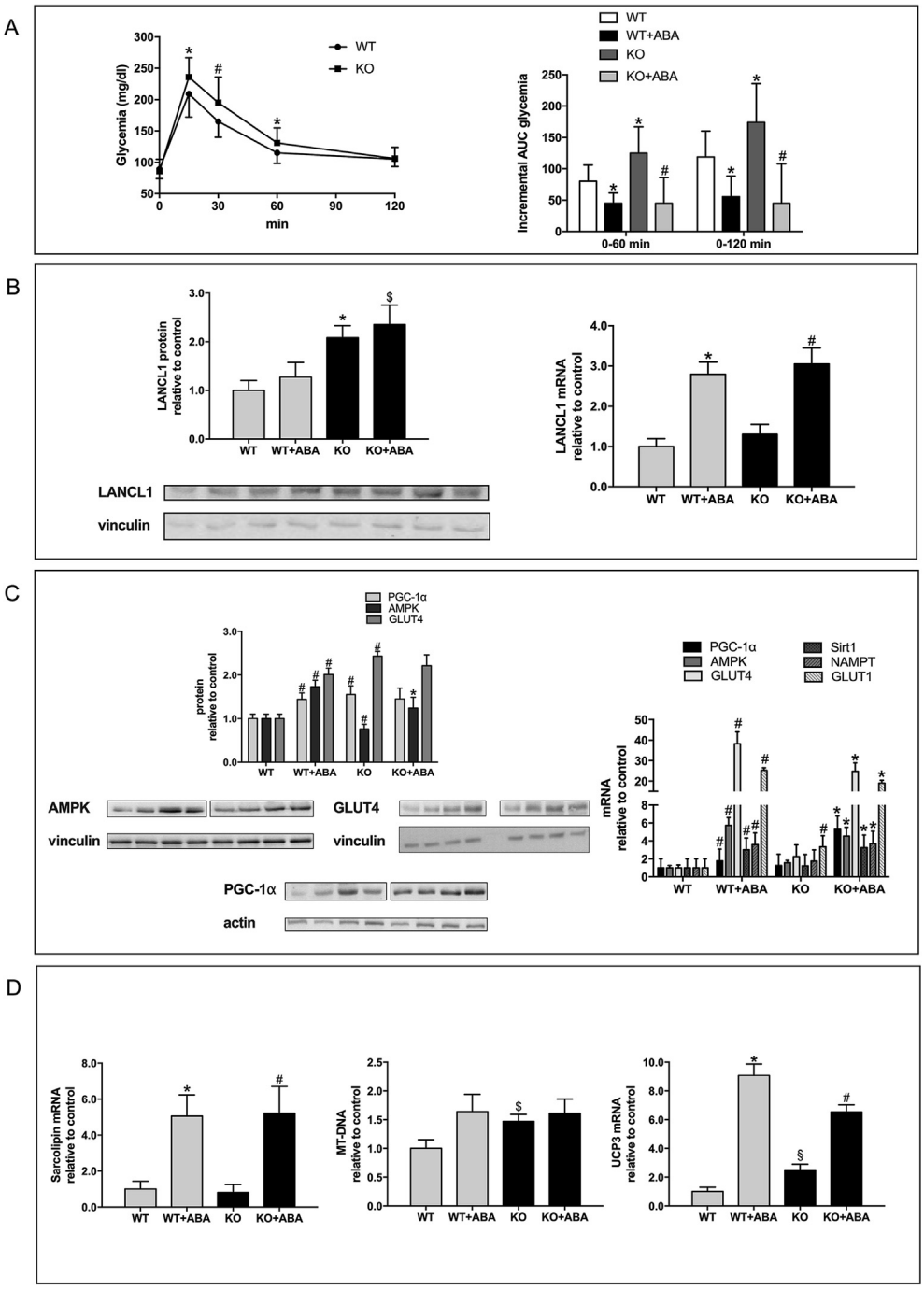

Figure 6: LANCL2$^{-/-}$ mice respond to ABA with an improved glucose tolerance *via* an increased transcription of GLUT4/GLUT1 and of the AMPK/PGC-1α/Sirt1 axis. A. Male, 7 week-old LANCL2$^{-/-}$ mice (KO) and their wild-type siblings (WT), 9 *per* group, were subjected to an oral glucose tolerance test (OGTT). *Left panel*, glycemia profile as monitored by tail vein puncture at the indicated time points after gavage. $^{*}p < 0.04$ and $^{\#}p < 0.01$ relative to WT. *Right panel*, incremental AUC of glycemia, calculated, in the indicated time frames, with the trapezoidal rule on the glycemia increase relative to time zero in WT and KO mice undergoing an OGTT with or without ABA at 1 μg/kg BW, in addition to glucose. $^{*}p < 0.05$ relative to WT; $^{\#}p < 0.003$ relative to KO. **B-D.** LANCL2$^{-/-}$ and WT mice were treated without or with ABA (1 μg/kg BW/day administered in the drinking water) for 4 weeks. At the end of treatment, mice were euthanized, and samples of skeletal muscle were taken for Western blot analysis and qPCR of the indicated proteins. Results shown are relative to the WT expression level and are the mean ± SD from 4 to 6 mice per group. P values are calculated by unpaired t-test. **B.** LANCL1 protein (*left panel*) and mRNA (*right panel*). A representative Western blot analysis is shown for $n = 2$ animals for each condition. $^{*}p < 0.05$ relative to WT; $^{\#}p < 0.02$ relative to KO; $^{\$}p < 0.05$ relative to ABA-treated WT. P values are calculated by unpaired two-tailed t-test. **C.** Protein expression (*left panel*) or mRNA transcription (*right panel*) of GLUT4, GLUT1, the AMPK/PGC-1α/Sirt1 signaling axis, and NAMPT are expressed relative to levels in untreated WT muscle. A representative Western blot analysis is shown for $n = 2$ animals for each condition. $^{\#}p < 0.05$ relative to WT; $^{*}p < 0.04$ relative to KO. P values are calculated by unpaired two-tailed t-test. **D.** Sarcolipin (*left panel*) and UCP3 (*right panel*) mRNAs and the mitochondrial DNA content (*central panel*), determined by qPCR on genomic DNA, are expressed relative to the respective content in WT mice (control). $^{*}p < 0.009$, $^{\$}p < 0.05$ and $^{\S}p < 0.01$ relative to WT; $^{\#}p < 0.004$ relative to KO. P values are calculated by unpaired two-tailed t-test.

further increases the expression of LANCL1 in the SM up to 3-fold over untreated WT levels (Figure 6B). Indeed, the overexpression of LANCL1 stimulates important metabolic functions in L6 myoblasts: glucose uptake (Figure 3), *via* an increased expression of GLUT4 and GLUT1 (Figure 3C), and O_2 consumption (Figure 5), *via* an increased expression of the uncoupling proteins sarcolipin and UCP3 (Figure 5A). In LANCL2$^{-/-}$ mice, in which the expression of LANCL1 in the SM is significantly higher than in WT mice, the same molecular effects are observed (i.e., the increased expression of GLUT4/1 [Figure 6C] and of sarcolipin and UCP3 [Figure 6D]). In addition, mitochondrial DNA is also increased, indicating a higher mitochondrial content in the SM from LANCL2$^{-/-}$ mice, particularly after treatment with ABA (Figure 6D). These effects appear to be mediated by the same master regulators activated by LANCL2 (i.e., AMPK and PGC-1α; Figure 6C). In addition, LANCL1 overexpression in both L6 cells and the SM from LANCL2$^{-/-}$ mice elicits an increased transcription of Sirt1 and NAMPT (Figures 3C and 6C). The AMPK/PGC-1α/Sirt1 axis is implicated in several pivotal functions in SM, including mitochondrial biogenesis and fusion, conservation of muscle contractility and recovery of muscle function caused by disuse or ageing [20], and protection of muscle cells from apoptosis induced by nutrient deprivation or ischemia-reperfusion injury [27–29]. The overexpression of NAMPT in SM improves physical endurance in mice [24] and maintains mitochondrial NAD^+ levels, membrane potential, respiration, and cell survival to oxidative stress [23]. Thus, the role of LANCL1/2 and ABA in promoting the activity of the AMPK/PGC-1α/Sirt1/NAMPT axis adds new key players to this molecular pathway in SM physiology.

Why should there be more than one ABA receptor? There could be several non-mutually exclusive answers to this question: i) redundancy of a physiologically important receptor pathway; ii) tissue-specificity of LANCL1/2 expression, mediating different, cell-specific functions of these proteins; iii) multiplicity of signaling pathways downstream of LANCL1 *vs.* LANCL2, activating different functional responses in the same cell.

Given the relevant role of ABA as an insulin-independent stimulator of cell glucose uptake *via* an increased expression of both GLUT 4 [11,30] and Figure 3 and GLUT 1 (Figure 3), receptor redundancy may be interpreted as a protective mechanism to safeguard ABA-responsiveness and glucose entry into cells, even in the face of one receptor mutation or genetic ablation. Indeed, as ABA is present in both the plant and animal kingdoms, it has evolved as a hormonal signal stimulating cell glucose uptake much earlier than insulin. Screening the genome databases for the reported association between SNPs in LANCL1 (or LANCL2) and specific clinical phenotypes does not produce many results. Interestingly, the LANCL1 gene lies within the Insulin-dependent diabetes (Idd) 5.3 locus, which provides resistance to T1D in NOD mice [30]. LANCL1 is also among the candidate genes responsible for an observed complex phenotype of impaired neuronal function due to a microdeletion on the chromosomal region 2q34 [31]. However, the overlapping functions of LANCL1 and LANCL2 on glucose transport and mitochondrial respiration unveiled in this study suggest that both proteins may need to be mutated to observe a significant phenotype. LANCL3, the third member of the LANCL protein family, is, indeed, expressed at a much lower level compared to the other two LANCL proteins (Figure 6C S). Regarding receptor function redundancy, it may be relevant to observe that a transcriptional control appears to link LANCL1 and LANCL2 in both L6 cells and *in vivo* in LANCL2$^{-/-}$ mice. In L6 cells, in which the expression of LANCL2 or LANCL1 were silenced, significantly increased mRNA levels of the other LANCL protein were observed (Figure 7S). In LANCL2$^{-/-}$ mice, mRNA levels of LANCL1 were significantly higher relative to those in WT mice, in both the SM (Figure 6B) and the BAT (19.5 ± 12.7 vs. 1.0 ± 0.7, $n = 3$, $p < 0.03$).

It is also possible that different tissue expression levels of LANCL1 and LANCL2 could mediate a tissue-specific function of these proteins, either ABA-related or −unrelated. However, LANCL1 and LANCL2 are both similarly and highly expressed in the CNS (Figure 6A,B S), whereas the glucose transporters present on neuronal cells comprise GLUT1 and GLUT4, both targets of LANCL1/2-mediated increased expression. Heart and germinal cells follow the brain in the ranking of the tissues with the highest LANCL1/2 expression level (Figure 6B S). It could be argued that these tissues are essential to species and individual survival.

Both LANCL1 and LANCL2 bind to reduced glutathione (GSH) and have an SH3-binding domain (a highly conserved protein−protein interaction domain). These features have been proposed to allow these proteins to sense the cell redox state and be actors in response to its dysregulation. Indeed, it has been reported that loss of LANCL1 leads to neuronal death, oxidative stress, and inflammation in the brain, whereas LANCL1 overexpression protects neurons against exogenous peroxide-induced apoptosis [32]. In addition, LANCL1 overexpression protects motor neurons from apoptosis in mice with a genetic mutation of SOD, a model of amyotrophic lateral sclerosis, possibly by activating Akt [33]. The biochemical mechanism underlying the protective effect of LANCL1, particularly regarding a possible role for LANCL1 in stimulating glucose transport/mitochondrial respiration, remains to be investigated but should be attempted in light of the findings presented here. Another observation pointing to a protective role of LANCL1 in neuronal cells comes from an *in vitro* study on a model of neuronal cell death caused by oxygen- and glucose-deprivation. The overexpression of LANCL1 reduced cell death through a signaling pathway dependent on Akt, PGC-1α, and Sirt3 activation [34]. Our observation that the overexpression of either LANCL1 or LANCL2 similarly increases cell respiration, sarcolipin, and UCP3 expression in rat L6 cells and that their combined silencing dramatically reduces mitochondrial DNA and the expression of sarcolipin and UCP3 (Figure 5) are consistent with the general role of these proteins in stimulating cell glucose transport and mitochondrial respiration *via* an AMPK/PGC-1α-dependent mechanism (Figures 4, 5 and [8]). In addition, a significant correlation exists between the level of (over) expression of LANCL1 or LANCL2 in L6 cells and the extent of increase of cell O_2 consumption (Figure 5B). The overexpression of PGC-1α in the SM has been shown to increase cell respiration [35]. The high expression level of LANCL1/2 in the brain may be related to this effect on mitochondria.

LANCL1 has been shown to bind to the SH3 domain of the signaling protein Eps8, thereby allowing for the nerve growth factor-induced neurite outgrowth in the model neuronal cells PC12 [36]. Interestingly, this feature is also shared by LANCL2, another possible example of functional redundancy of the LANCL proteins. Recent reports indicate that LANCL2 may also be involved in the protection of neurons against oxidative stress, possibly through its capacity to bind glutathione (thus, responding indirectly to the redox state of the cell) and its ability to interact with several proteins involved in kinase-dependent signaling (mTORC, Akt, AMPK) and gene transcription. No clear distinction between the functional effect of the overexpression of LANCL1 *vs.* LANCL2 emerged from our study, suggesting that either one can similarly stimulate glucose uptake and cell respiration in L6 myoblasts. Some of the functional features attributed to one of the proteins have not yet been concomitantly explored in the other one; thus, it is possible that further functional overlapping exists. One function attributed to LANCL2, in which LANCL1 shared no role, is the effect of LANCL2 overexpression or silencing on developing

preadipocytes. In this study, the authors show that LANCL2, but not LANCL1, activates the PPAR-γ-mediated transactivation of adipogenic genes in 3T3L1 murine preadipocytes induced to differentiate with insulin and dexamethasone [10].

It should be noted that, in the absence of insulin, the overexpression of LANCL2 does not induce adipocyte differentiation and that the overexpression of LANCL2 sensitizes cells to the adipogenic effect of insulin [11], possibly *via* the activation of the mTORK/Akt pathway. Thus, this insulin-sensitizing feature may be a distinguishing property between LANCL2 and LANCL1, though this tentative conclusion needs further study. Most recently, modified gut microbiota was observed in LANCL1$^{-/-}$ mice compared to wild-type animals, an alteration the authors suggest may alleviate the oxidative damage to the brain, which they expected, but did not observe [37]. The possibility that LANCL2 vicariated the function of LANCL1 in these mice.

Regarding the signaling pathways downstream of LANCL1 and LANCL2, there are again several reports indicating shared features. Akt, AMPK, PGC-1α, and Sirtuins 1 and 3 lie downstream of LANCL2 and LANCL1 [8,9,11,34] and this report. Increased AMPK activity could, in theory, result from an increased ratio between pAMPK and total pAMPK or from an increased protein expression of AMPK with an unchanged ratio between the phosphorylated and the unphosphorylated protein. The ABA-LANCL1/2 system acts through the latter mechanism in both LANCL1/2 overexpressing L6 cells and LANCL1 overexpressing LANCL2 KO mouse muscle.

Ex vivo treatment of skeletal muscle samples from WT mice for 30 or 60 min with 100 nM ABA also increased Sirt6 mRNA levels 2.33 ± 0.06 and 2.55 ± 0.11 times, respectively, more than levels in untreated samples ($n = 3$; $p < 0.0001$). Interestingly, Sirt6 deletion in adipose tissue impairs the thermogenic function of brown adipose tissue (BAT), causing a "whitening" of brown fat. Conversely, Sirt6 overexpression in primary fat cells stimulates browning [38]. In mice with a muscle-specific Sirt6 deficiency, impaired glucose homeostasis, insulin sensitivity, and reduced physical performance are observed [39]. Our results and literature data warrant an in-depth exploration into the role of the ABA/LANCL1-2 system in the activation of muscle and BAT Sirt6.

Interestingly, increased transcription of TBC1D1 was also observed in L6 cells overexpressing either LANCL1 or LANCL2, compared to control cells infected with the empty vector (1.31 ± 0.05 and 1.39 ± 0.08 relative to control, $n = 3$, $p < 0.01$ for both values). The RabGAPs TBC1D1 and TBC1D4 are key signaling factors in skeletal muscle glucose utilization. In mice, deficiency of both RabGAPs reduces skeletal muscle glucose transport in response to insulin and lowers GLUT4 abundance. Both RabGAPs are targets of AMPK: TBC1D1 appears to control exercise endurance by maintaining high muscle glucose uptake after contraction, and TBC1D4 improves muscle insulin sensitivity after contraction [40,41]. Thus, these proteins are among those responsible for the beneficial effect of physical exercise on blood glucose control in insulin-resistant or −deficient subjects.

The increased transcription of TBC1D1 observed in L6 cells overexpressing LANCL1 or LANCL2 warrants further studies to explore a possible correlation between the expression levels of the LANCL proteins and of TBC1D1/4. A clear correlation exists between the expression levels of LANCL1 and LANCL2 and mRNA levels, along with protein expression and plasmamembrane translocation of GLUT1 and GLUT4 (Figure 4).

LANCL2 has been shown to translocate to the nucleus, particularly upon ABA binding [7]. The possible nuclear translocation of LANCL1 has not been explored in this study and to our knowledge has not been described in other reports.

The results presented here indicate an overlapping of downstream signaling proteins activated by both LANCL2 and LANCL1, both *in vitro* in L6 myoblasts overexpressing one or the other LANCL proteins (Figure 3C—D and 4) and *in vivo*, in the SM of LANCL2$^{-/-}$ mice (Figure 6C). Expression of LANCL1 in the SM from LANCL2$^{-/-}$ mice was higher compared to that in WT (Figure 6B) and was further increased, particularly at the mRNA level by ABA treatment of the mice, as also occurred in WT animals (Figure 6B, right panel). Plasma ABA (ABAp) was similar in WT and LANCL2$^{-/-}$ mice; thus, the increased expression of LANCL1 in ABA-untreated LANCL2$^{-/-}$ mice cannot depend on a higher ABAp. Instead, it could be hypothesized that LANCL2 controls to some extent LANCL1 transcription and that the hormone itself is part of this regulatory network, possibly by promoting the nuclear translocation of its receptor(s).

The existing literature, taken together with the results reported in this study, reveals a complex picture of the pleiotropic functions of LANCL1 and LANCL2 in mammalian physiology. LANCL1 appears to be involved in cell (particularly muscle) glucose uptake and mitochondrial respiration and cell (particularly neuronal) survival to low oxygen/nutrient availability and oxidative stress. It remains to be assessed whether these survival-related functions may be affected *via* ABA binding. As ABA is present in the serum, complete cell culture media contain nanomolar ABA. Thus, cells cultured with an animal serum-containing medium will have been in contact with ABA during culture, if not during the experimental condition (which may have been performed in protein-free media). Here we show that LANCL1/2-overexpressing cells cultured with nanomolar ABA for 24 h and then resuspended in serum- and ABA-free buffers have a significantly higher oxygen consumption than ABA-untreated cells. *Ex vivo* incubation of the SM from WT mice with nanomolar ABA for 60 min resulted in a 15-fold overexpression of NAMPT (Figure 4 S). Thus, the effect of ABA on mitochondrial respiration and NAD^+ synthesis, and possibly on other cellular functions as well, can persist for hours after the removal of the hormone and can be fast. Interestingly, ABA is particularly abundant in the brain, with concentrations of approx. 1 log higher compared to other tissues [42]. It is possible that the distinctive and unifying feature of their ABA-binding capacity makes the LANCL proteins part of an ancestral mechanism of stress response to changing conditions of nutrient/oxygen availability, mitochondrial respiration, and ROS generation. The particular abundance of LANCL1/2 (and ABA) in the brain may be related to their role in individual and species survival.

AUTHOR CONTRIBUTIONS

SS and GB: methodology, biochemical and molecular biology data curation and visualization; LG: methodology, biochemical data curation; MM: *in vivo* data curation (animal experimentation); DG and CD: *in vitro* biophysical data curation (DC); CS, LI, and HDJ: *in vitro* biophysical data curation (SPR); EZ and LS: conceptualization, funding acquisition, project administration, writing, editing

FUNDING

This work was supported by the University of Genova funds to EZ and LS.

CONFLICT OF INTEREST

The authors declare no conflict of interest.

APPENDIX A. SUPPLEMENTARY DATA

Supplementary data to this article can be found online at https://doi.org/10.1016/j.molmet.2021.101263.

REFERENCES

[1] Li, B., Yu, J.P.J., Brunzelle, J.S., Moll, G.N., Van der Donk, W.A., Nair, S.K., 2006. Structure and mechanism of the lantibiotic cyclase involved in nisin biosynthesis. Science 311:1464–1467.

[2] Eley, G.D., Reiter, J.L., Pandita, A., Park, S., Jenkins, R.B., Maihle, N.J., et al., 2002. A chromosomal region 7p11.2 transcript map: its development and application to the study of EGFR amplicons in glioblastoma. Neuro-Oncology 4: 86–94.

[3] He, C., Zeng, M., Dutta, D., Koh, T.H., Chen, J., Van der Donk, W.A., 2017. LanCL proteins are not involved in lanthionine synthesis in mammals. Scientific Reports 7:40980.

[4] Sturla, L., Fresia, C., Guida, L., Bruzzone, S., Scarfì, S., Usai, C., et al., 2009. LANCL2 is necessary for abscisic acid binding and signaling in human granulocytes and in rat insulinoma cells. Journal of Biological Chemistry 284: 28045–28057.

[5] Magnone, M., Sturla, L., Guida, L., Spinelli, S., Begani, G., Bruzzone, S., et al., 2020. Abscisic acid: a conserved hormone in plants and humans and a promising aid to combat prediabetes and the metabolic syndrome. Nutrients 12:E1724.

[6] Landlinger, C., Salzer, U., Prohaska, R., 2006. Myristoylation of human LanC-like protein 2 (LANCL2) is essential for the interaction with the plasma membrane and the increase in cellular sensitivity to Adriamycin. Biochimica et Biophysica Acta 1758:1759–1767.

[7] Fresia, C., Vigliarolo, T., Guida, L., Booz, V., Bruzzone, S., Sturla, L., et al., 2016. G-protein coupling and nuclear translocation of the human abscisic acid receptor LANCL2. Scientific Reports 6:26658.

[8] Magnone, M., Emionite, L., Guida, L., Vigliarolo, T., Sturla, L., Spinelli, S., et al., 2020. Insulin-independent stimulation of skeletal muscle glucose uptake by low-dose abscisic acid *via* AMPK activation. Scientific Reports 10:1454.

[9] Zeng, M., Van der Donk, W.A., Chen, J., 2014. Lanthionine synthetase C-like protein 2 (LanCL2) is a novel regulator of Akt. Molecular Biology of the Cell 25: 3954–3961.

[10] Dutta, D., Lai, K.Y., Reyes-Ordoñez, A., Chen, J., Van der Donk, W.A., 2018. Lanthionine synthetase C-like protein 2 (LanCL2) is important for adipogenic differentiation. Journal of Lipid Research 59:1433–1445.

[11] Sturla, L., Mannino, E., Scarfì, S., Bruzzone, S., Magnone, M., Sociali, G., et al., 2017. Abscisic acid enhances glucose disposal and induces brown fat activity in adipocytes *in vitro* and *in vivo*. Biochimica et Biophysica Acta 1862: 131–144.

[12] Kubista, M., Sjöback, R., Eriksson, S., Albinsson, B., 1994. Experimental correction for the inner-filter effect in fluorescence spectra. Analyst 119:417–419.

[13] Crouse, H.F., Potoma, J., Nejrabi, F., Snyder, D.L., Chohan, B.S., Basu, S., 2012. Quenching of tryptophan fluorescence in various proteins by a series of small nickel complexes. Dalton Transactions 41:2720–2731.

[14] Cea, M., Cagnetta, A., Adamia, S., Acharya, C., Tai, Y.T., Fulciniti, M., et al., 2016. Evidence for a role of the histone deacetylase SIRT6 in DNA damage response of multiple myeloma cells. Blood 127:1138–1150.

[15] Livak, J., Schmittgen, T.D., 2001. Analysis of relative gene expression data using real- time quantitative PCR and the $2^{-\Delta\Delta CT}$ method. Methods 25:402–408.

[16] Bruzzone, S., Ameri, P., Briatore, L., Mannino, E., Basile, G., Andraghetti, G., 2012. The plant hormone abscisic acid increases in human plasma after hyperglycemia and stimulates glucose consumption by adipocytes and myoblasts. The FASEB Journal 26:1251–1260.

[17] Cichero, E., Fresia, C., Guida, L., Booz, V., Millo, E., Scotti, C., et al., 2018. Identification of a high affinity binding site for abscisic acid on human Lanthionine synthetase component C-like protein 2. The International Journal of Biochemistry & Cell Biology 97:52–61.

[18] Datta, D., Swamy, J.M., 2017. Fluorescence and circular dichroism studies on the accessibility of tryptophan residues and unfolding of a jacalin-related α-d-galactose-specific lectin from mulberry (Morus indica). Journal of Photochemistry and Photobiology B 170:108–117.

[19] Lee, J.O., Lee, S.K., Jung, J.H., Kim, J.H., You, G.,Y., Kim, S.J., et al., 2011. Metformin induces Rab4 through AMPK and modulates GLUT4 translocation in skeletal muscle cells. Journal of Cellular Physiology 226:974–981.

[20] Petrocelli, J.J., Drummond, M.J., 2020. PGC-1α-Targeted therapeutic approaches to enhance muscle recovery in aging. International Journal of Environmental Research and Public Health 17:8650.

[21] Vidal-Puig, A., Solanes, G., Grujic, D., Flier, J.S., Lowell, B.B., 1997. UCP3: an uncoupling protein homologue expressed preferentially and abundantly in skeletal muscle and brown adipose tissue. Biochemical and Biophysical Research Communications 235:79–82.

[22] Halling, J.F., Pilegaard, H., 2020. PGC-1α-mediated regulation of mitochondrial function and physiological implications. Applied Physiology Nutrition and Metabolism 45:927–936.

[23] Yu, A., Zhou, R., Xia, B., Dang, W., Yang, Z., Chen, X., 2020. NAMPT maintains mitochondria content via NRF2-PPARalpha/AMPKalpha pathway to promote cell survival under oxidative stress. Cellular Signalling 66:109496.

[24] Costford, S.R., Brouwers, B., Hopf, M.E., Sparks, L.M., Dispagna, M., Gomes, A.P., et al., 2018. Skeletal muscle overexpression of nicotinamide phosphoribosyl transferase in mice coupled with voluntary exercise augments exercise endurance. Molecular Metabolism 7:1–11.

[25] Sturla, L., Fresia, C., Guida, L., Grozio, A., Vigliarolo, T., Mannino, E., et al., 2011. Binding of abscisic acid to human LANCL2. Biochemical and Biophysical Research Communications 415:390–395.

[26] Magnone, M., Ameri, P., Salis, A., Andraghetti, G., Emionite, L., Murialdo, G., et al., 2015. Microgram amounts of abscisic acid in fruit extracts improve glucose tolerance and reduce insulinemia in rats and in humans. Federation of American Societies for Experimental Biology Journal 29(12):4783–4793.

[27] Yu, Y., Zhao, Y., Teng, F., Li, J., Guan, Y., Xu, J., et al., 2018. Berberine improves cognitive deficiency and muscular dysfunction via *act*ivation of the AMPK/SIRT1/PGC-1α pathway in skeletal muscle from naturally aging rats. The Journal of Nutrition, Health & Aging 22:710–717.

[28] Ma, L., Wang, R., Wang, H., Zhang, Y., Zhao, Z., 2020. Long-term caloric restriction activates the myocardial SIRT1/AMPK/PGC-1α pathway in C57BL/6J male mice. Food & Nutrition Research 29:64.

[29] Tang, J., Lu, L., Liu, Y., Ma, J., Yang, L., Li, L., et al., 2019. Quercetin improves ischemia/reperfusion-induced cardiomyocyte apoptosis in *vitro an*d in *vivo st*udy via *SI*RT1/PGC-1α signaling. Journal of Cellular Biochemistry 120: 9747–9757.

[30] Hunter, K., Rainbow, D., Plagnol, V., Todd, J.A., Peterson, L.B., Wicker, L.S., 2007. Interactions between Idd5.1/Ctla4 and other type 1 diabetes genes. The Journal of Immunology 179:8341–8349.

[31] Westphal, D.S., Andres, S., Makowski, C., Meitinger, T., Hoefele, J., 2018. MAP2 - a candidate gene for epilepsy, developmental delay and behavioral abnormalities in a patient with microdeletion 2q34. Frontiers in Genetics 45: 927–936.

[32] Huang, C., Chen, M., Pang, D., Bi, D., Zou, Y., Xia, X., et al., 2014. Developmental and activity-dependent expression of LanCL1 confers antioxidant activity required for neuronal survival. Developmental Cell 30:479–487.

[33] Tan, H., Chen, M., Pang, D., Xia, X., Du, C., Yang, W., 2020. LanCL1 promotes motor neuron survival and extends the lifespan of amyotrophic lateral sclerosis mice. Cell Death & Differentiation 27:1369–1382.

[34] Xie, Z., Cao, B.-Q., Wang, T., Lei, Q., Kang, T., Ge, C.-Y., et al., 2018. LanCL1 attenuates ischemia-induced oxidative stress by Sirt3-mediated preservation of mitochondrial function. Brain Research Bulletin 142:216—223.

[35] Zhang, L., Zhou, Y., Wu, W., Hou, L., Chen, H., Zuo, B., et al., 2017. Skeletal muscle-specific overexpression of PGC-1α induces fiber-type conversion through enhanced mitochondrial respiration and fatty acid oxidation in mice and pigs. International Journal of Biological Sciences 13: 1152—1162.

[36] Zhang, W., Wang, L., Liu, Y., Xu, J., Zhu, G., Cang, H., et al., 2018. Structure of human lanthionine synthetase C-like protein 1 and its interaction with Eps8 and glutathione. Genes & Development 23:1387—1392.

[37] Zhang, F., Qi, N., Zeng, Y., Bao, M., Chen, Y., Liao, J., et al., 2020. The endogenous alterations of the gut microbiota and feces metabolites alleviate oxidative damage in the brain of LanCL1 knockout mice. Frontiers in Microbiology 11:557342.

[38] Yao, L., Cui, X., Chen, Q., Yang, X., Fang, F., Zhang, J., et al., 2017. Cold-inducible SIRT6 regulates thermogenesis of Brown and beige fat. Cell Reports 20(3):641—654.

[39] Cui, X., Yao, L., Yang, X., Gao, Y., Fang, F., Zhang, J., et al., 2017. SIRT6 regulates metabolic homeostasis in skeletal muscle through activation of AMPK. American Journal of Physiology - Endocrinology And Metabolism 313(4):E493—E505.

[40] Kjøbsted, R., Roll, J.L.W., Jørgensen, N.O., Birk, J.B., Foretz, M., Viollet, B., et al., 2019. AMPK and TBC1D1 regulate muscle glucose uptake after, but not during, exercise and contraction. Diabetes 68(7):1427—1440.

[41] Espelage, L., Al-Hasani, H., Chadt, A., 2020. RabGAPs in skeletal muscle function and exercise. Journal of Molecular Endocrinology 64(1):R1—R19.

[42] Le Page-Degivry, M.T., Bidard, J.N., Rouvier, E., Bulard, C., Lazdunski, M., 1986. Presence of abscisic acid, a phytohormone, in the mammalian brain. Proceedings of the National Academy of Sciences 83:1155—1158.

